Hessam Moussavinik

On Narrowband Interference Mitigation Methods for Robust Wireless Sensor Networks

Thesis for the degree of Philosophiae Doctor

Trondheim, March 2013

Norwegian University of Science and Technology
Faculty of Information Technology, Mathematics and Electrical Engineering
Department of Electronics and Telecommunications
and in collaboration with
Intervention Center, Oslo University Hospital

NTNU – Trondheim
Norwegian University of
Science and Technology

NTNU
Norwegian University of Science and Technology

Thesis for the degree of Philosophiae Doctor

Faculty of Information Technology, Mathematics and
Electrical Engineering
Department of Electronics and Telecommunications
and in collaboration with
Intervention Center, Oslo University Hospital

ISBN 978-82-471-4265-3 (printed ver.)
ISBN 978-82-471-4267-7 (electronic ver.)
ISSN 1503-8181

Doctoral theses at NTNU, 2013:83

Printed by NTNU-trykk

To my beloved wife,
Sara
and my lovely children,
Anahita and Armin.

Abstract

In this dissertation different approaches to robustness in ultra wideband (UWB) wireless sensor networks, specifically biomedical applications, are studied. UWB wireless sensor networks are unlicensed users of the frequency spectrum and they can be interfered by signals from other licensed users/devices that are generally narrowband signals. Due to the relatively high power of narrowband interferences (NBI) UWB wireless sensor networks can strongly get affected and loose their performance. This problem is addressed in the thesis along methods to make UWB wireless sensor networks robust against NBI.

The discussed methods mainly come in two categories. One category suggests methods for a blind UWB wireless sensor network, and by *blind* we mean that the network has no knowledge about its proximity and NBI. Signaling schemes, frequency interleaving, scheduling and modulation are discussed in this category. The next category suggests using feedback and keeping the UWB sensor network out of blindness. In this regard a method for enabling feedback in ultra wideband spectrum is studied. It should be mentioned that methods discussed in these two categories can get combined although they are named under two categories.

Results show that in a blind system, multiband signaling scheme with frequency interleaving and support of error correction codes can highly increase robustness of the system against NBI. Looking at multiuser scenario, a scheduling policy that is fair to all users and provides a steady

state to the system is found via Nash equilibrium. The proposed modulation shows that it is capable of inherently recovering some errors that occur due to NBI. When it comes to using feedback, the proposed methods, comprising compressed sensing and algebraic detector, provide good advantages regarding complexity and performance.

Thus in a bigger picture, the thesis studies the mentioned problem in UWB wireless sensor networks from different aspects and the proposed methods suggest practical solutions to the problem. Significantly the discussed methods can be combined together to overcome the problem under different conditions.

Preface

This dissertation is submitted in partial fulfillment of the requirements for the degree of Philosophiae Doctor (PhD) at the Department of Electronics and Telecommunications, Norwegian University of Science and Technology (NTNU), under supervision of Professor Ilangko Balasingham and co-supervision of Professor Tor Ramstad.

The PhD requirement at NTNU comprises of research, a year of full-time compulsory courses, and some teaching duties.

As a PhD student, I had the valuable chance of having visiting research appointment abroad. In the first half of year 2010, I was at EURECOM in Sophia-Antipolis, France, working in collaboration with Professor Awatif Hayar.

The work included in this thesis has been funded by the SAMPOS WISENET Project, which is funded by the Research Council of Norway under the contract number 176875/S10 and 176724/I30. The stay at EURECOM was funded by the VERDIKT Programme of The Research Council of Norway. The teaching duties has been funded by the Department of Electronics and Telecommunications, NTNU.

Acknowledgements

Working on Ph.D. has been a great experience. I am indebted to several people for making the time working on my Ph.D.

First of all, I am deeply grateful to my advisor Ilangko Balasingham. To work with you has been a real pleasure to me. You have oriented and supported me with promptness and care.

Furthermore, I am very grateful to my co-advisor Tor A. Ramstad. Thank you for your insightful comments, for your support and for all motivating discussions we had.

I would also like to thank Geir E. Øien and Niels D. Aakvaag as my other inspiring co-advisors. During my Ph.D. I had the opportunity of visiting EURECOM institute in Sophia Antipolis, France. There I had the chance to work with Aawatif Hayar and Wael Guibène. Thanks to Awatif for her great inspirations and guidance and thanks to Wael for his great collaboration.

In addition, I have been very privileged to get to know and to collaborate with many other great people who became friends over the last several years. Over the last few years, Sang-Seon Byun has been a faithful friend and co-author. Thank you for teaching me so much and for the interesting discussions we had. I also want to thank Babak Moussakhani, Luxmiram Vijayandran, John Torjus Flåm, Mehdi Soufifar, Rodrigo de Miguel, Nurul Hoda Mahmood, and Solomon Tesfamicael for their great friendship, and all the interesting discussions we had.

I would also like to thank my parents and my parents in law for their support. Many thanks to my mother in law, Soheila Roshdieh, for her great support with my family that I could finish writing this thesis.

Finally, I am greatly thankful to Sara Hajikazemi, my wonderful wife, for her love, support and patience during the last several years. You are the light of my life. Thank you with all my heart!

Contents

List of Tables

List of Figures

Abbreviations

AD	Algebraic detection/detector
ADC	Analog to digital converter
AWGN	Additive white Gaussian noise
BER	Bit error rate
BPPM	Binary pulse position modulation
BPSK	Binary phase shift keying
BWSN	Biomedical wireless sensor network
CCK	Complementary code keying
CFD	Cyclostationary features detector
COFDM	Coded orthogonal frequency division multiplexing
CR	Cognitive radio
CS	Compressive sampling / Compressed sensing
dB	Decibel
DVB-T	Digital video broadcasting-terrestrial
ECG	Electrocardiogram
ED	Energy detector
EEG	Electroencephalography
FCC	Federal communications commission
FEC	Forward error correction
GFSK	Gaussian frequency shift keying

IEEE	Institute of electrical and electronics engineers
IR-UWB	Impulse radio-ultra wideband
ISM	Industrial-scientific-medical
LLR	Log likelihood ratio
M-QAM	M-ary quadrature amplitude modulation
MMSE	Minimum mean square error
NAR	NBI to AWGN Ratio
NBI	Narrowband interference
NE	Nash equilibrium
NTNU	Norwegian University of Science and Technology
O-QPSK	Offset quadrature phase shift keying
OFDM	Orthogonal frequency division multiplexing
OOK	On-off keying
PAM	Pulse amplitude modulation
PPFM	Pulse position and frequency modulation
PPM	Pulse position modulation
PSD	Power spectral density
PSK	Phase shift keying
PU	Primary user
QPSK	Quadrature phase shift keying
QRE	Quantal response equilibrium
ROC	Receiver operating characteristics
SIR	Signal to interference ratio
SNR	Signal to noise ratio
SU	Secondary user
TR-UWB	Transmitted reference-ultra wideband

UWB	Ultra wideband
UWB-RT	Ultra wideband-radio technology
Wi-Fi	Wireless fidelity
WLAN	Wireless local area network
WSN	Wireless sensor network

Notations

$\lvert\cdot\rvert$	Absolute value
$\lVert\cdot\rVert$	Norm
$\lvert$	Given
$(\cdot)^{-1}$	Matrix inversion
$\mathbf{x}^*$	Conjugate transpose
$\mathbf{x}^\mathbb{T}$	Transpose
$<,>$	Group
$\{,\}$	Set
$\in$	Set membership
$\ll$	Much less than
$:=$	Equal by definition
$\times$	Cartesian product
$\mathcal{H}$	Hypothesis

Chapter 1

Introduction

Wireless sensor networks (WSNs) may be a potential instrument for improving many aspects of life quality. They have a wide range of applications, for example from simple environment monitoring to vital data collection and controlling. We should keep in mind that by WSNs we mainly refer to short range WSNs. An specific example on their application could be biomedical wireless sensor network (BWSN) or body area network (BAN), where sensors in such a network are used as biological indicators to monitor health of humans or other living organisms and creatures. For example sensors can be used for electroencephalography (EEG), electrocardiogram (ECG), blood pressure measurement, etc. Sensors can be of different types where some are wearable and some of them may get implanted in the body. With this biomedical application, BWSN can be used to continuously monitor elderly people, and people under recovery, while they lead their normal life. As another example, BWSN can remove many wires of medical sensing equipments attached to the body while in hospital. This makes it more tidy and easy for any action. Based on the application of WSN the restrictions on the performance of the network changes. Considering the BWSN that is used on humans, high performance, reliability and stability are required. BWSN should be able to work without any defect at required reliability, whenever and wherever. Of course when we say 'whenever and wherever' it lies in a defined range of operating conditions, as it is the case for any device. In this context we

look at techniques of implementation of wireless sensor networks, existing challenges, and we approach one of the challenges, i.e. mitigating narrowband interference, using different proposals.

The rest of this chapter is organized as following. Section 1.1 describes implementation techniques for wireless sensor networks with a comparative view. Section 1.2 presents the basics of ultra wideband (UWB) radio technology. In section 1.3 existing challenges within UWB wireless sensor networks are discussed. Section 1.4 briefly explains the scope of this dissertation. Contributions of the thesis is mentioned in section 1.5. Finally, section 1.6 presents an overview on the thesis and shows the focus of each chapter.

1.1 Short Range Wireless Sensor Network

A wireless sensor network can be implemented with different techniques or protocol standards, such as Bluetooth, ZigBee, UWB, and Wi-Fi. These protocols are implementations of the IEEE 802.15.1, 802.15.4, 802.15.3, and 802.11a/b/g/ standards, respectively. A brief introduction and comparison to these protocols is in place before we pick one of them for further discussion.

Bluetooth is based on a wireless radio system designed for short range and cheap implementation to replace cables for computer peripherals, such as mice, etc. This range of applications is known as wireless personal area network (WPAN) [40]. ZigBee defines specifications for low rate WPAN in order to support simple devices which consume minimal power and typically operate in the personal operating space of 10m [40].

Ultra-Wideband (UWB) radio technology has been an interesting and attractive technique for indoor short range and high speed wireless communication, in recent years [40], [59]. Wireless fidelity (Wi-Fi) includes IEEE 802.11a/b/g standards for wireless local area networks (WLAN). It lets users surf Internet at broadband speeds when connected to an access point

or in ad hoc mode [40].

Now let us look at some of the differences among these protocols. In Table 1.1 some aspects of these protocols are compared. A higher data rate is provided by Wi-Fi and UWB compared to Bluetooth and ZigBee. The spacial range of Bluetooth, UWB and ZigBee is intended for wireless personal area network (WPAN) communication (about 10m), while Wi-Fi is oriented to wireless local area network (WLAN) communication, i.e. about 100m and is not short range in our context. Howsoever, ZigBee can also reach 100m in some applications [40].

The power spectral density emission limit for UWB transceivers is -41.3 dBm/MHz according to the Federal Communications Commission (FCC) regulations [61]. This is the same power limit that applies to unlicensed emitters in the UWB band. The nominal transmission power for Bluetooth and ZigBee is 0 dBm and for Wi-Fi is 20 dBm [40].

Comparing the data rate we note that UWB provides the highest data rate in short range communication. Therefore UWB is also very attractive for devices that require high data rate, e.g., audio and video applications [59].

Table 1.1: Side by side comparison of Bluetooth, ZigBee, UWB and Wi-Fi protocols, extracted from [40].

Standard Protocol	**Bluetooth**	**ZigBee**	**UWB**	**Wi-Fi**
IEEE spec.	802.15.1	802.15.4	802.15.3a	802.11a/b/g
Frequency band	2.4 GHz	868/915 MHz; 2.4 GHz	3.1-10.6 GHz	2.4 GHz; 5GHz
Max signal rate	1 Mb/s	250 Kb/s	110 Mb/s	54 Mb/s
Nominal range	10 m	10-100 m	10 m	100 m
Nominal TX power	0-10 dBm	(-25)-0 dBm	-41.3 dBm/MHz	15-20 dBm
Number of RF channels	79	1/10; 16	1-15	14 (2.4 GHz)
Channel bandwidth	1 MHz	0.3/0.6 MHz; 2 MHz	500 MHz - 7.5 GHz	22 MHz
Modulation Type	GFSK	BPSK (+ASK), O-QPSK	BPSK, QPSK	BPSK, QPSK, COFDM, CCK, M-QAM

In addition to the mentioned differences, it is very important to compare the energy consumption of the mentioned protocols. Figure 1.1 shows a comparison of the normalized energy consumption for each protocol. It can be seen that UWB offers the highest efficiency in energy consumption for short range communication. The second most efficient one is Wi-Fi, but as already mentioned it cannot be considered as short range communication in our context.

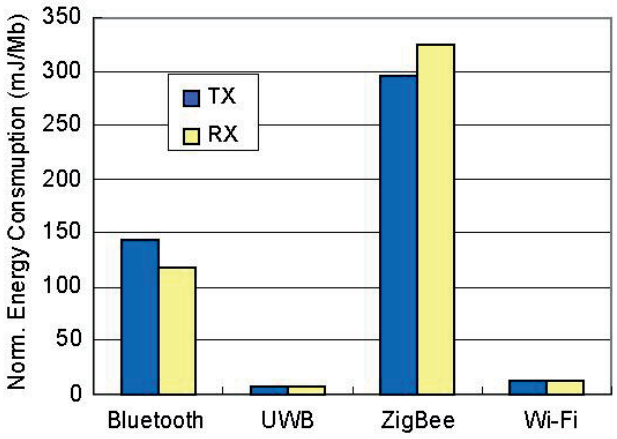

Figure 1.1: Comparison of the normalized energy consumption for each protocol [40].

Considering BWSN, we find that it requires medium data rate, since most of the medical signals have small bandwidth requirements [39]. Data rates up to 10 Mbps is often sufficient [42]. The range of operation in BWSN is short, typically between 2 to 5 meters [39, 42]. Also efficient power consumption is an important factor in BWSN or any other wireless network, where the power consumption profile affects the complexity and transmission power of the system [65]. Having these issues in mind, it is easy to infer that UWB would be one of the best choices for BWSN. For example, regarding the power efficiency, [15] presents a low power wireless signal transmitter for use with biomedical sensors in micro size based on UWB

radio technology.

Besides the type of protocol to use, a BWSN generally comes with a central topology where all sensors communicate with a central node, often called the fusion center. Usually, it is the fusion center that is responsible for most of the processing load. An example of a fusion center is a cell phone. For instance, a patient's cell phone collects all the data from sensors which are connected to his/her body, may or may not processes data, and sends it to a monitoring unit at a hospital through an available network (e.g., 3G, WiFi Internet).

1.2 Ultra Wideband Radio Technology

Since UWB is a strong candidate for BWSN, let us briefly review the history and properties of UWB radio technology.

Most of the initial concepts and patents for ultra wideband radio technology (UWB-RT) originated in the late 1960's. At that time, this technology was alternately referred to as baseband, carrier-free or impulse. The term "ultra wideband" was not applied to this technology until approximately 1989, when by that time, UWB theory, techniques and many hardware approaches had experienced well over 30 years of extensive development [24, 68]. Given the potential of UWB-RT for covert communication and ranging systems, as well as the lack of appropriate regulations regarding spectrum usage, the development and use of systems based on UWB-RT has been mainly the privilege of US military and government agencies. Nevertheless, the recent initiative taken by the FCC in the US to regulate the legal use of UWB radio devices have induced growing commercialization activities and also similar regulatory and research efforts in other parts of the world, e.g., Europe [77]. UWB regulation is necessary because the radio spectrum is a scarce resource (3 KHz - 300 GHz) where almost all portions are allocated for specific purposes. Accordingly, emerging wireless applications requires a share in the radio spectrum. Frequency can be reused at different times or in different geographical locations, when

permitted. The FCC regulations on UWB allow UWB devices to share the spectrum without disturbing others [5]. Figure 1.2 shows a concept of frequency reuse and sharing spectrum with UWB.

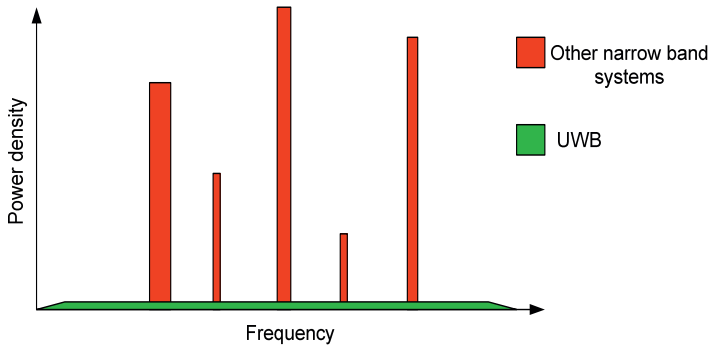

Figure 1.2: Frequency reuse concept with UWB sharing the spectrum [5].

The usable frequency range for UWB communication is different around the world, but in US it is [3.1 10.6] GHz where the allocated maximal power spectral density (PSD) is always -41.3 dBm/MHz [1]. Table 1.2 shows the UWB usable frequency ranges in different nations.

Table 1.2: Usable frequency ranges for UWB communication in different nations [1].

Nation	1st frequency band in GHz	2nd frequency band in GHz
USA	[3.1 10.6]	-
Europe	[4.2 4.8]	[6.0 8.5]
Japan	[3.4 4.8]	[7.25 10.25]
Korea	[3.1 4.8]	[7.2 10.2]
Singapore	[4.2 4.8]	[6.0 9.0]
China	[4.2 4.8]	[6.0 9.0]

The FCC has defined radio signals for UWB such that the fractional bandwidth of the signal, i.e. the ratio between the signal's bandwidth and center frequency, should be greater than 25%, and relative bandwidth should be over 500MHz, regardless of the fractional bandwidth. The bandwidth is measured at the upper and lower cuttoff points (-10dB), f_H and f_L, respectively, and the center frequency, f_C, is defined as the average of these cutoff points [77, 5].

$$\text{Fractional Bandwidth} = \frac{2(f_H - f_L)}{(f_H + f_L)} > 25\% \tag{1.1}$$

$$f_C = \frac{(f_H + f_L)}{2} \tag{1.2}$$

One of the popular and major techniques to implement UWB is impulse radio (IR) that is based on transmitting very short (e.g. 0.1-2 ns) and low power pulses. Use of IR technique can eliminate the requirement for up-conversion and down-conversion which reduces the transceiver complexity. Possible modulation schemes for IR-UWB can be on-off keying (OOK), pulse amplitude modulation (PAM), pulse position modulation (PPM), and phase shift keying (PSK), while receivers can be based on energy detector and rake receivers [3, 77]. UWB is capable to provide high data rates in short ranges with low cost and simple transceivers [31]. UWB can operate with single-band or multi-band signaling schemes [3].

The benefits and characteristics claimed for systems based on UWB-RT are as follows [77, 5, 13]:

- ◇ Extremely low power spectral density (PSD).
- ◇ Spectrum reuse, i.e., ability to share the frequency spectrum with narrowband signals.
- ◇ Less sensitive to multipath effects: the short pulses potentially allow differentially delayed multipath components to be distinguished at the receiver with the benefit that a reduced fading margin may be applied in a system's link budget analysis.
- ◇ Simple transceiver structure.
- ◇ Multiuser communication.

- ◇ Extremely high data rates are possible.
- ◇ Fine time resolution.

With the UWB properties a wide range of wireless applications become possible, such as:

- ○ Wireless personal area network (WPAN), e.g., replacing cables between multimedia consumer electronics devices [5]. In [17] some motivations of UWB-RT for high data rate WPAN applications are presented.
- ○ Indoor positioning and localization [84, 62, 71].
- ○ UWB for radio frequency identification (UWB RFID) [85].
- ○ Public safety applications, including motion detection in disaster situations [77].
- ○ Low data rate applications, e.g., sensors and home, office, and medical automation [36].

The next section describes some of the existing challenges in UWB WSN.

1.3 Challenges within UWB Short Range WSN

In this section we discuss some of the challenges when implementing a short range WSN, e.g. BWSN or BAN, based on UWB radio technology. UWB offers a promising solution to an overcrowded frequency spectrum, but since UWB frequency spectrum is within the unlicensed Industrial, Scientific, Medical (ISM) band, coexistence with other narrowband systems becomes an important issue [21]. Coexistence is defined as "the ability of one system to perform a task in a given (shared) environment where other systems may or may not be using the same set of rules " [14]. In other words, the capability of handling the interference from other devices, where most of them are narrowband systems, is required. Although the interfered frequencies by narrowband systems are a small fraction of the UWB spectrum, but since the NBI signal has relatively much higher power spectral density than the UWB signal it is inevitable that UWB

receivers suffer degradations in range, capacity, and bit error rate [3, 27].

Much research on the methods to mitigate interferences between different wireless communication systems is presently conducted. For example, in [12] coexistence between different wireless systems operating in 2.4GHz ISM band is discussed and interference mitigating methods based on traffic scheduling techniques are proposed. They consider particularly IEEE 802.11 wireless local area networks (WLANs) and Bluetooth (BT) nodes. In [48] a power control algorithm is proposed to mitigate interference in an environment with high density 802.11 networks. [80] talks about interference mitigation for body area networks and proposes several interference mitigation schemes such as adaptive modulation, adaptive data rate and duty cycle. Also in [66] the impact of narrowband interference signals on impulse radio ultra wideband communication systems is investigated and it is shown that the NBI from IEEE 802.11a can severely degrade the UWB bit error rate performance.

Mitigating interference is an important mechanism to improve communication reliability in BAN or BWSN [32]. Therefore one of the major concerns with UWB for BWSN is to cope with the strong narrowband interferences (NBIs). Generally, there are two main strategies for dealing with NBI, namely avoiding and canceling methods. Avoiding and canceling can result in a better performance when they are used together, however, if the exact information about the center frequency of the NBI is not known, then suppressing NBI is not possible by use of the avoidance techniques[3, 78]. As an example in [57] a detect and avoid approach is used for a elderly-care monitoring sensor system with UWB radio technology. In some situations and for some reasons a device may not be able to detect the center frequency of an existing NBI. For example, in order to reduce the complexity of each biomedical sensor, which has a limited source of power, sensors may not be equipped with the spectrum detection ability. In this context NBI is unknown to the UWB device (e.g., sensor with UWB transmitter).

If detecting NBI within the UWB spectrum is demanded, other challenges arise. The very first and an important one is the sampling challenge due to

the wide spectrum of UWB. The traditional sampling frequency, according to Nyquist sampling theorem, is at least twice the highest frequency in the signal, and in bandpass signals between two and four times its bandwidth. Therefore, sampling the UWB spectrum requires a very high sampling rate. This high sampling rate may be too high due to the level of process restrictions and limitations in technology of analog-to-digital converters (A/D) and the cost of high-rate A/D [44, 37, 6]. In this regard, finding other methods of data acquisition and processing are very important. Compressive sensing (CS) makes it possible to reconstruct a *sparse* signal by taking less samples than Nyquist sampling, and thus wideband spectrum sensing is doable by CS [73, 34].

Another challenge within any WSN is power consumption of sensors. Sensors have a limited source of power, and it is not feasible to change their batteries often. Specially, consider that a sensor is implanted in a human body. Then it would not be feasible at all to change the battery within short periods. Also, for networks that have a lot of sensors around a large area, it is not practical to change the power source of the sensors. This makes it necessary to look for a system that is as energy efficient as possible. Figure 1.1 indicates that UWB is the most efficient protocol in this regard.

Along with all the mentioned challenges, UWB communication has been regarded as the strongest candidate for short range wireless network due to its inherent beneficial properties, e.g., robustness against severe multipath jamming, excellent time resolution, and low power transmission [3, 55, 39, 42, 65]. Moreover, UWB communication can be operated in a multiband fashion including adaptive selection of the frequency subbands to provide high robustness against NBI, and to provide more efficient usage of the FCC spectral mask [3, 55].

1.4 Scope of the thesis

Up till now, we have become familiar with short range wireless networks based on UWB radio technology and some of the challenges in implementing such networks. Let us now describe the scope of the thesis to point

out the topics that are discussed in more detail throughout this thesis.

As it is already seen, reliability and robustness against NBI in a BWSN based on UWB radio technology are very important. Robustness and reliability are the basis for the discussions in this thesis. We will discuss mitigating unknown NBI in a BWSN that is based on UWB radio technology. When we say unknown NBI, it means that the BWSN has no information about NBI through detection or any other way. We propose a technique based on multiband signaling scheme and forward error correction coding (FEC) to make the sensor network more robust against unknown NBI.

The proposed technique for mitigating NBI, has great multiuser capabilities in a way that several sensors can communicate simultaneously while all of the sensors can experience the same robustness in their communication. We will present a schedule for multi sensor (user) communication via a game theoretic approach. The schedule makes it possible for all the sensors to have a same experience of robustness against NBI during their communication.

Next, a modulation technique is proposed. This modulation and its receiving algorithm is able to handle unknown NBI and recover some errors inherently.

Further improvement of reliability in a wireless network may require higher complexity. For example if we consider that sensors in a network provide feedback about the spectrum to the fusion center, we make the network more complex in the hope of reaching a better reliability. Here, we face a tradeoff between more robustness and complexity in the system. Thus, in order to enable feedback in the network, the sensor nodes (or some of them) should be given the ability of sensing the spectrum in their vicinity. This also defines the concept of cognitive radio. But, as it is mentioned earlier, sampling the wide spectrum of UWB is a big challenge and hard to achieve on each sensor. Therefore, in this thesis we look for a technique

to simplify the sampling task via compressive sensing techniques. Then, an algebraic method is applied on the obtained samples to detect NBI. Furthermore, we also discuss the cooperative detection scenario.

1.5 Contributions of the Thesis

This thesis contributes to UWB wireless sensor networks communications with the following proposals.

- A design principle for practical UWB wireless sensor networks with low complexity and high robustness against unknown NBI.
- A scheduling policy that keeps the proposed multiuser system in a steady state and sensors have fairly equal access to the resources.
- A new modulation that is inherently able to correct some errors that are occurred due to NBI.
- A method for enabling feedback in UWB sensors network by use of compressed sensing and an algebraic detector. The proposed method has relatively low complexity and is very effective in wideband spectrum sensing.

1.6 Structure of the Thesis

The rest of this thesis has the following structure.

Chapter 2 ***Blind Interference Mitigation in UWB-WSN:*** This chapter proposes a method for handling narrowband interference (NBI) that does not require any exact information about the center frequency of NBI. The proposed method uses a combination of forward error correction (FEC) codes and a scheduled multi-band UWB scheme. The method performs well in dealing with NBI and in environments with unknown or variable NBI. The work of this chapter is published in [50].

Chapter 3 ***Robustness in Multiuser UWB Communications:*** In this chapter we extend the multiband IR-UWB scheme to multiuser scenarios, where the UWB frequency band can be accessed by multiple users (sensors) simultaneously. We find a steady state condition where all the users achieve a required performance while each user handles the NBI such that other users can also achieve the required performance, while none of the users change its action in order to gain more performance. This chapter presents a game theoretic approach for finding the steady state which also dictates the multiuser transmission schedule. The work of this chapter is published in [51] and [54].

Chapter 4	***Robustness via Modulation:*** This chapter introduces a method to mitigate interference based on a new modulation technique which is simple and also works well when NBI signal is strong. Based on pulse position modulation (PPM) we propose pulse position and frequency modulation (PPFM) combination as the new modulation with inherent error correction capabilities. Then, we define a receiving algorithm for PPFM modulated signal that is able to mitigate strong narrow-band interferences. The proposed method is a general technique which can be used in multiband wireless communication systems. The work of this chapter is published in [49].
Chapter 5	***Feedback in UWB Wireless Sensors Network with Compressed Sensing*** This chapter presents a wireless sensor network where feedback is enabled. In this chapter we develop a combined compressive sampling and distribution discontinuities detection technique based on algebraic method for the sensing task of identifying the spectrum holes. A proper sensing matrix template is found. Also a centralized implementation of collaborative compressed sensing of wideband spectrum for cognitive radios that is combined with distribution discontinuities detection technique is proposed. The work of this chapter is published in [52] and [28].
Chapter 6	***Conclusion & Future Work*** This chapter presents conclusion and possible future works.

Appendix A ***UWB Pulse Design Algorithm:*** This appendix presents the used UWB pulse design algorithm as proposed in [58].

Chapter 2

Blind Interference Mitigation in UWB-WSN

2.1 Introduction

In this chapter a method for handling narrowband interference (NBI) that does not require any exact information about the center frequency of NBI is proposed. The proposed method uses a combination of forward error correction (FEC) codes and a scheduled multi-band UWB scheme. The method performs well in dealing with NBI and in environments with unknown or variable NBI. The work of this chapter is published in [50].

The rest of this chapter is organized as following. Section 2.2 describes the state of the art and background for the work presented in this chapter. Section 2.3 explains the proposed methods. Section 2.4 shows the simulation results for proposed methods. Section 2.5 discusses about the mentioned techniques and challenges. Conclusion is presented in section 2.6.

2.2 State-of-the-art

Coexistence of an ultra wideband wireless sensor network (UWB-WSN) with other wireless networks, and specially with narrow bandwidth signals, is an important issue to fulfill. There are two main strategies for dealing with NBI, namely avoiding and canceling methods [3]. The avoidance techniques are based on spectrum nulling or creating notch frequencies [43, 67], spectral-encoded UWB system [38, 18], or neglecting the frequency band that has major NBI, e.g. in OFDM by turning off the corresponding carrier [3]. For example, [83] presents design of UWB pulse to mitigate multiple NBI through combining several Gaussian derivative pulses with proper combination coefficients. [69] describes UWB waveform design based on raised cosine pulse for suppressing NBI. However, if the exact information about the center frequency of the NBI is not known, then its suppressing is not possible by use of the avoidance techniques [3]. Regarding the canceling techniques, typical used methods are the MMSE and RAKE receiving processing, and adaptive filtering technology [3, 41]. The avoidance and canceling techniques work best together [3]. Coexistence in general meaning includes effects from any type of network in proximity. For example separate UWB networks which mutually affect each other should be able to coexist. In this regard there are other techniques in use such as low duty-cycle (LDC) algorithm, presented in [70], that can reduce the average interference to the existing radio systems by lowering pulse repetition interval or pulse occupation time in BAN.

2.3 Methods

This chapter explains methods that are proposed for handling unknown NBI in UWB-WSN. It means that the UWB-WSN would be able to handle NBI without requiring information about center frequency of NBI. Such a method can then also handle time variable NBI. Below the assumed system and channel model is described followed a description of the methods.

2.3.1 System and Channel Models

A UWB system can be implemented by impulse radio techniques which offer very interesting features. Impulse radio has properties that make it a viable candidate for short-range communications in dense multipath environments [79]. In impulse radio techniques baseband pulses of very short time duration, in the order of nano seconds, are transmitted. The system becomes interesting since it is carrierless and its implementation cost is low [18, 37]. Some of the potential advantages of impulse radio UWB (IR-UWB) are low power consumption, high immunity against interference, low power spectral density, high data rate, adaptability to the electromagnetic environment in the human body, etc [30].

Data bits are modulated by binary pulse position modulation (BPPM). The reason for selection of BPPM is that under weak channel conditions, lower order modulation is preferred for low data rate applications [3]. In BPPM the first slot of the frame is reserved for bit value 1 and the last slot is reserved for bit value 0, where the proper pulse is transmitted over the corresponding slot. The BPPM signal modulation can be represented as following:

$$x(t) = p_{tr}(t - \delta d_b), \qquad d_b = \begin{cases} 0 & (b = 1) \\ 1 & (b = 0) \end{cases} \tag{2.1}$$

where $x(t)$ is the modulated signal to be transmitted, p_{tr} is the pulse shape of the UWB signal, δ is PPM fixed parameter that specifies the amount of shift in position and d_b gets its value according to the bit, b, to be transmitted [55]. We designed and used pulse shapes according to the algorithm described in [58], where the spectrum of the designed pulse fits with the frequency mask, according to the rules provided by the FCC. The pulse design algorithm is given in Appendix A.

The channel is assumed to be AWGN with existence of NBI. This NBI can have any center frequency within the UWB band, since our proposed system works irrespective of the position of NBI. We assumed NBI to be in the unlicensed national information infrastructure (U-NII)/industrial,

scientific and medical (ISM) frequency band, since 802.11a WLAN devices work in this band and these devices can be found almost everywhere.

At the receiver, matched filtering and energy detection followed by a hard decision are used. It is assumed to have perfect passband filters at the receiver. Figure 2.1 shows a general block diagram of this system model. In case of using forward error correction (FEC) codes, an encoder is used before the modulator at the transmitter side, and a decoder is used after the demodulator at the receiver side. The hard decision block will also be removed, where the decision is made at the end of the decoding procedure on the log-likelihood ratio (LLR) values. Figure 2.2 shows a general block diagram of the system model when FEC codes are used. Receivers are noncoherent and synchronized.

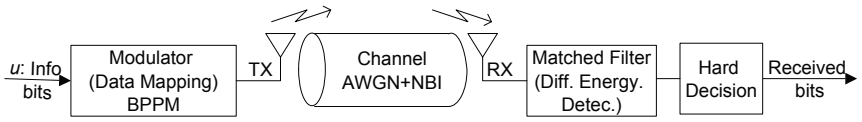

Figure 2.1: System model for IR-UWB with BPPM modulation

Figure 2.2: System model for IR-UWB with BPPM modulation and FEC coding

2.3.2 Single-band IR-UWB Scheme

In single-band signaling scheme, the spectrum of the impulse signal fits with the entire frequency mask of UWB. Figure 2.3 shows the spectrum of single-band scheme for UWB system.

Assume that the transmitted signal is sampled at the receiver with N points. Thus we represent the transmitted signal by a vector of its samples as $\mathbf{x}$ and the observed signal is given by

$$\mathbf{y} = \mathbf{x} + \mathbf{w} + \mathbf{s} \tag{2.2}$$

where $\mathbf{y}$, $\mathbf{w}$ and $\mathbf{s}$ are the vectors of samples of the observed signal, AWGN and NBI, respectively.
Since the transmitted pulse shape is completely known at the receiver, matched filtering is used. By means of matched filters we find the inhabited energy in the first and the last slots of each frame. By comparing the found energies, decision on the received bit is made. For simplicity of notation, let us denote the observed signal at the first and the last slot of the kth frame by $\mathbf{y}_{1k}$ and $\mathbf{y}_{0k}$, respectively. Assume $b = 1$ is transmitted

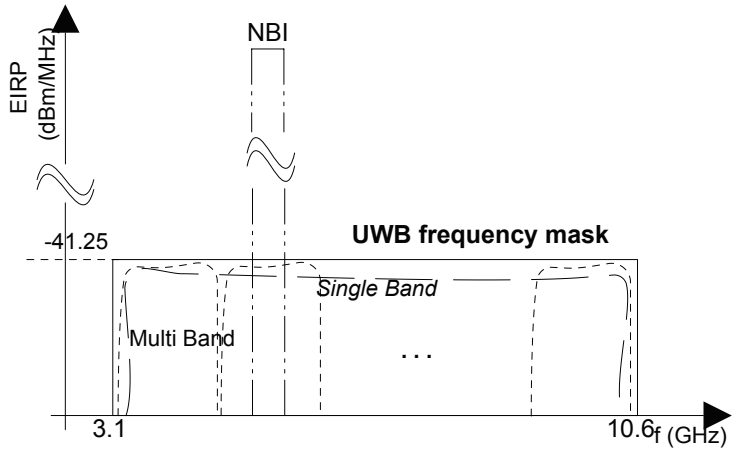

Figure 2.3: Frequency mask of UWB with spectrum of single- and multi-band signaling schemes

at the kth frame, then we have:

$$F_{1k} = \sum_{i=0}^{N-1} \mathbf{y}_{1k_i}.\mathbf{x}_{k_i} = \sum_{i=0}^{N-1} (\mathbf{x}_{k_i} + \mathbf{w}_{1k_i} + \mathbf{s}_{1k_i}).\mathbf{x}_{k_i}$$
$$= ||\mathbf{x}_k||^2 + \sum_{i=0}^{N-1} \mathbf{w}_{1k_i}.\mathbf{x}_{k_i} + \sum_{i=0}^{N-1} \mathbf{s}_{1k_i}.\mathbf{x}_{k_i} \tag{2.3}$$

$$F_{0k} = \sum_{i=0}^{N-1} \mathbf{y}_{0k_i}.\mathbf{x}_{k_i} = \sum_{i=0}^{N-1} \mathbf{w}_{0k_i}.\mathbf{x}_{k_i} + \sum_{i=0}^{N-1} \mathbf{s}_{0k_i}.\mathbf{x}_{k_i} \tag{2.4}$$

$$\tilde{b}_k = \begin{cases} 1 & , \quad F_{1k} > F_{0k} \\ 0 & , \quad \text{otherwise} \end{cases} \tag{2.5}$$

$$||\mathbf{x}_k||^2 = \sum_{i=0}^{N-1} |\mathbf{x}_{k_i}|^2 \tag{2.6}$$

where sums are on N sample points of a symbol, $\tilde{b}_k$ represents received bit at the kth frame, F_{1k} and F_{0k} are the amount of the inhabited energy found in the first and the last slot of the kth frame, respectively.

2.3.3 Multi-band IR-UWB Scheme

For multi-band signaling schemes the entire spectrum of UWB is divided into smaller bands of the minimum allowed bandwidth of 500 MHz [2]. The number of sub-bands and their bandwidth distribution is arbitrary and can be selected according to the application. We choose to have each subband with 500 MHz bandwidth. Thus, for the UWB spectrum, which is from 3.1 to 10.6 GHz, 15 subbands are obtained. Since we are interested in impulse radio signaling 15 different pulse shapes are required, where the spectrum of each one fits with one of the subband frequency masks.

Data bits can be sent in arbitrary ways over these subbands. We propose to send data bits serially in subsequent subbands. It means that bits can

be packed in strings of length 15 bits, and for each string we transmit the first, the second, and up to the fifteenth bit through the first, the second, and up to the fifteenth subband, respectively. This scheduling provides frequency interleaving.

2.3.4 IR-UWB, FEC and Frequency Interleaving Method

By equipping our conventional system with forward error correction (FEC) coding ability, the performance improves while the system complexity is increased a little. FEC is widely used in a big range of devices and communication systems. FEC increases the complexity but the performance gain it provides compensates for the additional complexity, and nowadays implementing FEC is considered as very basic. For the FEC coding we choose turbo product codes (TPC) with *a posteriori probability* (APP) iterative decoding algorithm. To keep the complexity relatively low a small Hamming$(8,4,4)^2$ product code is chosen. The rate of this code is $\frac{1}{4}$ with a minimum Hamming distance of 16 [53].

Figure 2.2 shows the system model with FEC coding. The information bits are encoded by the selected product code and the output of the encoder goes to the modulator as mentioned in Section 2.3.3. In some cases it may be useful to add an interleaver after the encoder. This has not been included in our model since it provides marginal increase in performance. Our decoding algorithm is a soft-in soft-out (SISO) algorithm. Therefore, we cannot do hard decision after demodulation as before. Proper soft input for the decoder is required. The mentioned decoder works for BPSK modulation, where the observed data would be the input to the decoder. In BPPM, similar signals are sent for both $b = \{0,1\}$ and only their positions are different within a frame, so they should be treated in another way. The decoder needs to consider two different phases for $b = 0$ and $b = 1$. So a differential energy detection is considered. We transmit $b = 1$ at the first and $b = 0$ at the last slot of a frame in BPPM and subtract the energy of the observed signal in the last slot from the energy of the observed signal in the first slot of each frame. This will give us a proper input for the

decoder. Assume $b = 1$ is transmitted in the kth frame. Then from (2.3) and (2.4) the differential energy can be derived:

$$F_{1k} - F_{0k} = ||\mathbf{x}_k||^2 + \sum_{i=0}^{N-1} (\mathbf{w}_{1k_i} - \mathbf{w}_{0k_i}).\mathbf{x}_{k_i} + \sum_{i=0}^{N-1} (\mathbf{s}_{1k_i} - \mathbf{s}_{0k_i}).\mathbf{x}_{k_i} \tag{2.7}$$

Similarly, if we assume that $b = 0$ is transmitted, we get

$$F_{1k} - F_{0k} = -||\mathbf{x}_k||^2 + \sum_{i=0}^{N-1} (\mathbf{w}_{1k_i} - \mathbf{w}_{0k_i}).\mathbf{x}_{k_i} + \sum_{i=0}^{N-1} (\mathbf{s}_{1k_i} - \mathbf{s}_{0k_i}).\mathbf{x}_{k_i} \tag{2.8}$$

This differential energy detection provides proper primary input data for the decoder. It is worth mentioning that the decoder uses LLR values to perform the iterations and from the final LLR values the decoder concludes the received bits.

2.4 Results

In this section we present simulation results for the mentioned methods.

2.4.1 Single-band IR-UWB Scheme

For this simulation NBI is assumed to be provoked by 802.11a WLAN devices that operate in the frequency band [5.15,5.35] GHz [26]. The frame duration of BPPM is set to 5ns, and the pulse duration is 1ns. That means there are 5 time slots in each frame where a pulse is transmitted in the first or the last slot depending on the bit value. Figure 2.4 shows the simulation results for different values of NBI to AWGN energy ratio (NAR). It can be seen that the performance degrades by increasing the NBI energy. When the NBI to AWGN energy ratio is at 30dB big performance degradation is visible.

2.4.2 Multi-band IR-UWB Scheme

For this simulation we assume NBI to be the same as before and within the frequency band of fifth subband, [5.1,5.6] GHz. Here, the frame duration of BPPM is 30ns, which includes 5 equal time slots. Simulation results for this system is shown in Figure 2.4. It is obvious that in this situation the performance of the multi-band scheme is better than single-band scheme. This is because the NBI disturbs only one subband out of 15, or one bit out of every 15 bits. Equations (2.3) and (2.4) are valid only for the observed signal that occurs in the disturbed subband, here it is in the fifth one, and for the rest of the subbands we have $\mathbf{s} = \mathbf{0}$. We can also see that the performance of this scheme still decreases when the NBI to AWGN energy ratio increases, but it is not as much as the performance degradation in the single-band scheme. This shows the advantage of using frequency interleaving.

2.4.3 Single-band IR-UWB Scheme with FEC

Simulations for a single-band scheme as shown in Figure 2.2 is performed. Figure 2.5 shows the simulation result. We can see that the performance of this scheme is better than the case without FEC. However, this is not surprising since the increase in performance is due to the coding gain. It is clear that by increasing the NBI to AWGN energy ratio, BER performance degrades. Although FEC is increasing the performance, but still this scheme is vulnerable to strong NBI.

2.4.4 Multi-band IR-UWB Scheme with FEC and Frequency Interleaving

This method is supposed to increase the robustness of the system against NBI better than the other discussed methods. The system model is shown in Figure 2.2 with a multi-band signaling scheme. Information bits are encoded and then transmitted by BPPM within subsequent frequency bands as explained in section 2.3.3. The multi-band transmitting schedule provides frequency interleaving. Figure 2.5 shows the simulation results of the

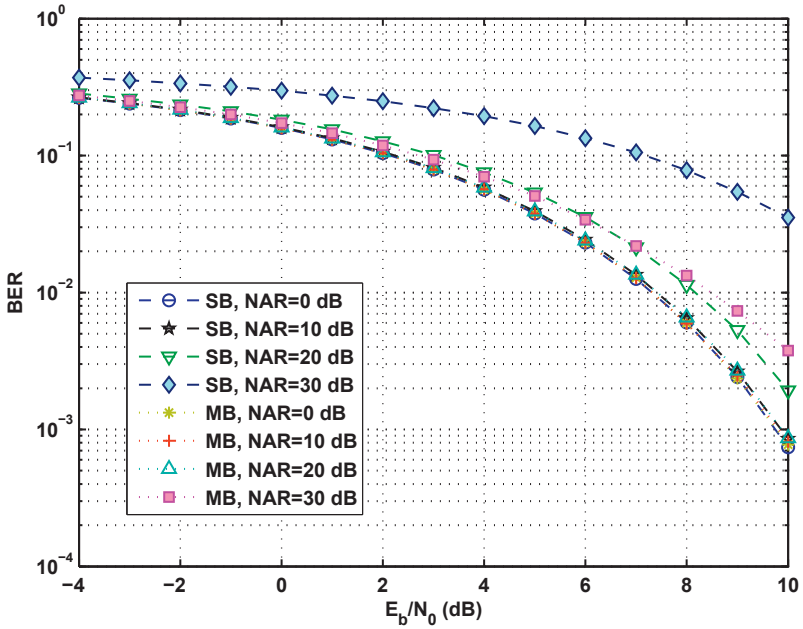

Figure 2.4: Performance of single- and multi-band (SB, MB, respectively) signaling schemes in AWGN channel with NBI. NAR: NBI to AWGN energy Ratio. E_b: Energy per information bit. N_0: AWGN energy.

system. The performance degradation with regards to NBI strength is low compared to the single-band scheme. If we compare both graphs, where the NBI to AWGN energy ratio is equal to 30 dB, we see that there is a big gap between these two performance curves, which is about 3.5dB gain in terms of $\frac{E_b}{N_0}$. The multi-band scheme is much more robust against NBI than the single-band scheme. The robustness and good performance is a result of the cooperation between FEC coding and frequency interleaving.

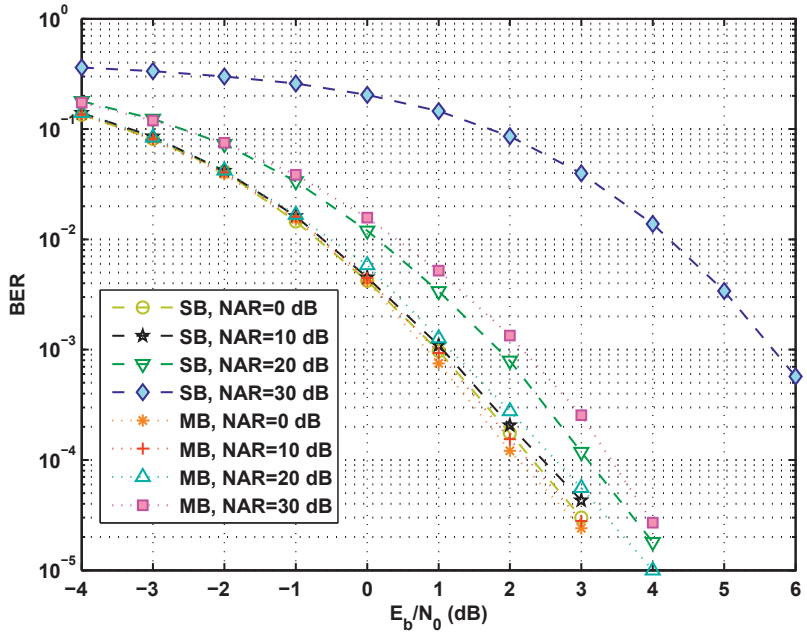

Figure 2.5: Performance of single- and multi-band (SB, MB, respectively) signaling schemes in AWGN channel with NBI. FEC codes with the APP decoding algorithm are used. Decoder performed 3 iterations. NAR: NBI to AWGN energy Ratio. E_b: Energy per information bit. N_0: AWGN energy.

2.5 Discussion

Different methods for handling NBI are proposed and simulated. Comparing the results multi-band IR-UWB scheme shows better robustness against NBI than the single band scheme. And to increase the performance further, FEC coding is a great addition to the system. A combination of multi-band scheme and FEC coding provides a rigorous frequency interleaving feature which results in a robust and effective system that is less sensitive to NBI. Also this combination makes the system able to perform well in situations where there is no knowledge about NBI avail-

able or the NBI is unknown or variable. It is also expected that the effect of combining FEC coding with multi-band scheme becomes more visible when there are more than one NBI source.

Using the multi-band scheme combined with FEC coding for one user per transmission period may seem to be wasteful in terms of using available resources or degrees of freedom. However, in a multiuser scenario this technique becomes more useful and efficient.

2.6 Conclusion

A technique is proposed to increase robustness of IR-UWB system in co-existence of narrowband interference (NBI). Simulation results show that cooperation of FEC coding and frequency interleaving using multi-band scheduling scheme, improves the robustness of the system. Another important contribution of this technique is that it does not require any prior information about the center frequency of NBI. Therefore it performs well in situations with *unknown* NBI or situations with variable NBI.

Chapter 3

Robustness in Multiuser UWB Communications

3.1 Introduction

The preceding chapter proposed an impulse radio-ultra wideband (IR-UWB) scheme with multiband signaling and FEC coding, and it is shown that in single user case, our scheme is beneficial for achieving robustness against unknown NBI. In this chapter, we extend the scheme to multiuser cases where the UWB frequency band can be accessed by multiple users simultaneously, and we look for a multiuser transmission schedule in a way that all the users can access the resources equally and all of them can experience the same robustness against NBI in their communication. The work of this chapter is published in [51] and [54].

The remainder of this chapter is organized as following. Section 3.2 defines the problem and the ways to solve it. In section 3.3 we describe a game model that matches our defined problem and in section 3.4 we find a Nash equilibrium for that given strategic game. Section 3.5 states the result and finally section 3.6 concludes this chapter.

3.2 Problem Definition

We extend the multiband IR-UWB scheme to multiuser senario, where the UWB frequency band can be accessed by multiple users simultaneously. We want to find a state where all the users achieve a required performance while each user handles the NBI such that other users can also achieve the required performance, and none of the users wants to change its action in order to gain more performance. In other words, all the users form a group which works in a steady state.
Different methods can be used to find schedules such as list scheduling, dynamic programming, mathematical programming, linear programming, etc. But for the problem at hand these methods may not offer the easiest solution. Furthermore, the given definition of steady state corresponds to Nash equilibrium of a mixed strategic non-cooperative game. Thus another way to find such a steady state is to look for a Nash equilibrium (NE) of a strategic game [56] that matches our problem. In this context, an n-transmitter Jamming game, an extended version of traditional jamming game [45], is the game that states our case well. Therefore we choose to use the existing game instance and adapt it for our problem to find the steady state. The game is explained here and we find a Nash equilibrium for such a game. The result of the Nash equilibrium provides us with a scheduling policy.

3.3 Game Model: n-Transmitter Jamming Game

Prior to describing the game model, the following assumptions are made:

- UWB frequency band consists of equally divided m subbands;
- let n denote the number of transmitters;
- every transmitter transmits a single bit by each pulse.

Following notations in [56], we model the n-transmitter jamming game that consists of

- ◇ a finite set of players $N = \{0, \cdots, n\}$, i.e. one jammer (player 0) and n transmitters (player $1, \cdots,$ player n);

  $A_i = \{a_{i1}, \cdots, a_{iJ_i}\}$: the set of actions available to each player i with J_i pure strategies;

- ◇ $A = \times_{i \in N} A_i$: the set of strategy profiles of the players;
- ◇ $\Delta(A_i)$: the set of probability distributions over A_i;
- ◇ u_i: utility function of player i on A, $u_i : A \to \mathbb{R}$;
- ◇ $U_i : \times_{j \in N} \Delta(A_j) \to \mathbb{R}$ that assigns to each $\alpha \in \times_{j \in N} \Delta(A_j)$ the expected value under u_i of the lottery over A that is induced by α (so that $U_i(\alpha) = \sum_{a \in A} (\Pi_{j \in N} \alpha_j(a_j)) u_i(a)$ if A is finite).

This strategic game, that is the *mixed extension* of the strategic game $\langle N, (A_i), (u_i) \rangle$, is denoted as $\langle N, (\Delta(A_i)), (U_i) \rangle$. We refer to a member of A_i and $\Delta(A_i)$ as a *pure strategy* and *mixed strategy* of player i, respectively [56]. We consider that there are m channels (subbands) over the whole UWB frequency band, which are denoted by the set $S = \{s_1, \cdots, s_m\}$. Then the transmission using an available channel is each player's action, that is, $A_i = \{a_{is_1}, \cdots, a_{is_m}\}$ where a_{is_j} is binary and indicates that player i transmits using channel s_j. We define the pure strategic utility values with following rules.

- if any of the n transmitter is jammed by the jammer, i.e., they transmit over the same channel:
  - $u_{jammer} = 1$
  - $u_{jammed\_transmitter} = -1$
  - $u_{other\_transmitters} = 1$
- otherwise, i.e., if the jammer does not jam any transmitters:
  - $u_{jammer} = -1$
  - $u_{transmitters} = 1$

We denote the mixed strategies of player i by a vector $\alpha_i = (\alpha_{i_1}, \cdots, \alpha_{i_m})$ where $\alpha_{i_k} \geq 0$ for all $1 \leq k \leq m$, $\sum_{k=1}^{m} \alpha_{i_k} = 1$, and α_{i_k} is the probability

that player i uses its kth pure strategy. Then we define the mixed strategic utility for transmitter i as

$$U_{ij} = (1 \times \alpha_{D(-j)}) + (-1 \times \alpha_{Dj}) \text{ for } D \neq i, j \in \{1, \cdots, m\} \tag{3.1}$$

where Dj represents the jammer holding its jth strategy and $D(-j)$ represents the jammer holding its strategies other than its jth strategy, and for the jammer,

$$\begin{aligned} U_{Dj} = \quad & (1 \times \sum_{k=1}^{n} \binom{n}{k} \prod_{i=1}^{k} p_{ij} \prod_{l=k+1}^{n} (1 - p_{lj})) \\ + \quad & (-1 \times \prod_{i=1}^{n} (1 - p_{ij})) \quad \text{for } j \in \{1, \cdots, m\} \end{aligned} \tag{3.2}$$

where p_{ij} is the probability of transmitter i to select its jth strategy, and $\sum_{k=1}^{n} \binom{n}{k} \prod_{i=1}^{k} p_{ij} \prod_{l=k+1}^{n} (1 - p_{lj})$ indicates the probability of having k transmitters that have the same strategy with the jammer.

Consequently, the utility value in the n-transmitter jammer game gives the probability distribution over each player's action. Then we want to find a state where individual players cannot gain more utility by changing its action for itself, which is given by Nash equilibrium in a mixed strategic game [56].

3.4 Finding Nash Equilibrium

In this section we exploit *quantal response equilibrium* (QRE) [75, 46] that is defined as a statistical version of Nash equilibrium where each player is assumed to observe a noisy evaluation of the strategy values $U_{ij}(\alpha)$ of the form

$$\hat{U}_{ij}(\alpha) = U_{ij}(\alpha) + \epsilon_{ij}$$

where

$$U_{ij}(\alpha) = u_i(a_{ij}, \alpha_{-i})$$

is the expected utility to player i from playing its jth strategy, holding fixed its opponents' mixed strategies α_{-i}, and the ϵ_{ij} are random variables drawn according to some joint distribution. When the ϵ_{ij} follows an extreme value distribution (i.e., log Weibull distribution) with parameter λ, a *logistic quantal response equilibrium*, called also *Logit equilibrium*, is given by

$$\alpha_{ij} = \frac{e^{\lambda U_{ij}(\alpha)}}{\sum_{k=1}^{J_i} e^{\lambda U_{ik}(\alpha)}}.$$

It is proved that, when $\lambda \to \infty$, the Logit equilibria approach a unique Nash equilibrium of the underlying game, namely, *Logit solution* [75, 46]. We therefore can define the Logit equilibrium of transmitter i over its jth strategy as

$$\alpha_{ij} = \frac{e^{\lambda((1\times\alpha_{D(-j)})+(-1\times\alpha_{Dj}))}}{\sum_{k=1}^{m} e^{\lambda((1\times\alpha_{D(-j)})+(-1\times\alpha_{Dj}))}}, \tag{3.3}$$

and then its Logit solution is

$$\lim_{\lambda\to\infty} \alpha_{ij} = \lim_{\lambda\to\infty} \frac{e^{\lambda(\alpha_{D(-j)}-\alpha_{Dj})}}{\sum_{k=1}^{m} e^{\lambda(\alpha_{D(-j)}-\alpha_{Dj})}} = \frac{1}{m}. \tag{3.4}$$

Thus, all the transmitters' mixed strategies over each subband are equal to $\frac{1}{m}$, i.e., $p = p_{ij} = \frac{1}{m}$ for all $i \in \{1, \cdots, n\}$ and $j \in \{1, \cdots, m\}$.
Now, we consider the jammer and we have

$$\alpha_{Dj} = \frac{e^{\lambda(1\times\sum_{k=1}^{n}\binom{n}{k}p^k(1-p)^{n-k}+(-1\times(1-p)^n))}}{\sum_{k=1}^{m} e^{\lambda(1\times\sum_{k=1}^{n}\binom{n}{k}p^k(1-p)^{n-k}+(-1\times(1-p)^n))}} \tag{3.5}$$

and

$$\lim_{\lambda\to\infty} \alpha_{Dj} = \lim_{\lambda\to\infty} \frac{e^{\lambda(\sum_{k=1}^{n}\binom{n}{k}p^k(1-p)^{n-k}-(1-p)^n)}}{\sum_{k=1}^{m} e^{\lambda(\sum_{k=1}^{n}\binom{n}{k}p^k(1-p)^{n-k}-(1-p)^n)}} = \frac{1}{m}. \tag{3.6}$$

From (3.6) we see that the mixed strategy of the jammer is also $\frac{1}{m}$. Therefore, we find that letting all the transmitters have uniform probability of access to all m subbands, while the jammer also has uniform probability of access to all m subbands, is Nash equilibrium where no player can deviate its strategy for itself. This result gives a theoretical implication on the transmission scheduling that makes each sensor able to access all available subbands uniformly.

3.4.1 Example with Gambit Software: Nash Equilibrium of a 3-Transmitter Jamming Game

In this section we find a Nash equilibrium (NE) for a specific game with $n = 3$. In this game we have 3 transmitters, one jammer (NBI) and 4 subbands. In order to find a NE for this game we employ *Gambit* software, software tools for game theory, version 0.2007.12.04[47]. There are several available options in Gambit to find the NE. We use *tracing logit equilibria* option to find one NE for our defined strategic game. The found NE is shown in Table 3.1.

Table 3.1: NE for 3-transmitter Jamming game.

Players\ Mixed strategics	s_0	s_1	s_2	s_3
T_1	0.25	0.25	0.25	0.25
T_2	0.25	0.25	0.25	0.25
T_3	0.25	0.25	0.25	0.25
J	0.25	0.25	0.25	0.25

In Table 3.1, T_1, T_2 and T_3 are the three transmitters, J is the jammer (NBI), s_0 to s_3 are the actions available to each player and the cross section of action columns and player rows are the mixed strategic values for corresponding player and action.

The NE that is given by Table 3.1 tells us that in our game, when the NBI is unknown, we can have a steady state in our system when all the transmitters have a uniform access to all the subband resources.

3.5 Results

3.5.1 Simulation Model

For the simulation, we assume that data bits of each sensor (transmitter) are modulated with binary pulse position modulation (BPPM) as described in Section 2.3.1. We consider an AWGN channel that is interfered by an undetected narrowband communication system within the UWB frequency band. It is assumed that the narrowband communication system is IEEE 802.11 services whose frequency range is $5.15 - 5.35$ GHz.

At the receiver side, matched filtering and differential energy detection followed by hard decision process are deployed, and we assume non-coherent and synchronized receiver [50]. Figure 3.1 shows a general block diagram of this system.

We let UWB frequency band consist of equally divided 15 subbands, and assume that each sensor transmits a single bit using a single subband simultaneously while letting each subband occupied by only one sensor during each pulse duration. On the beginning of each pulse duration, we let sensors shift their transmission subband according to the scheduling policy. In order to evaluate the scheduling policy given by Nash equilibrium (henceforth we call *uniform access scheduling*), we compare it with the scheduling policy where only one sensor decides its transmitting subband with non-uniform probability while the other sensors follow the uniform access scheduling policy.

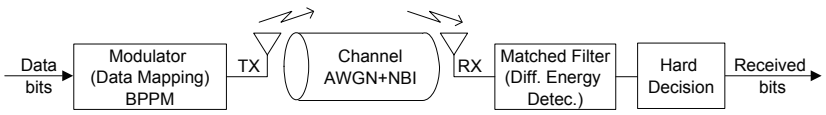

Figure 3.1: System model for IR-UWB with BPPM modulation.

The other assumptions to be made are as follows:

- The UWB frequency band ($3.1 - 10.6$ GHz) consists of equally divided 15 subbands, where the minimum allowed bandwidth of each subband is 500 MHz[2], i.e. 15 different pulse shapes are required.
- There is no NBI hopping.
- duration of $p_{tr} = 6 \times 10^{-9}$ sec.
- $\delta = 24 \times 10^{-9}$ sec.

3.5.2 Performance

First, we measure bit error rate (BER) at each sensor when the uniform access scheduling is applied. Figure 3.2 plots the measured results according to different signal to NBI power ratio (SIR). As expected, we observe that same BERs are measured at all the sensors.

Next, we let one sensor deviate from the uniform access scheduling, i.e., let that sensor choose its subband with non-uniform random probability while the other sensors follow the uniform access scheduling. Figure 3.3 shows BER measured at that sensor. We observe that BER of the sensor that deviates from the uniform access scheduling becomes larger than the one measured when it follows the uniform access scheduling. Therefore, we confirm that no single sensor can gain more benefit for itself by deviating from the scheduling policy given by Nash equilibrium.

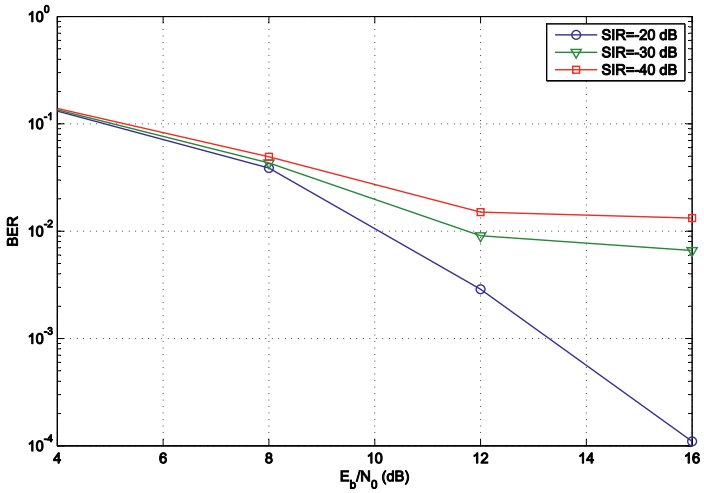

Figure 3.2: Bit error rate (BER) measured at all the sensors when the *uniform access scheduling* is applied. $\frac{E_b}{N_0}$ is energy per bit to AWGN power ratio, and SIR is Signal to NBI power ratio.

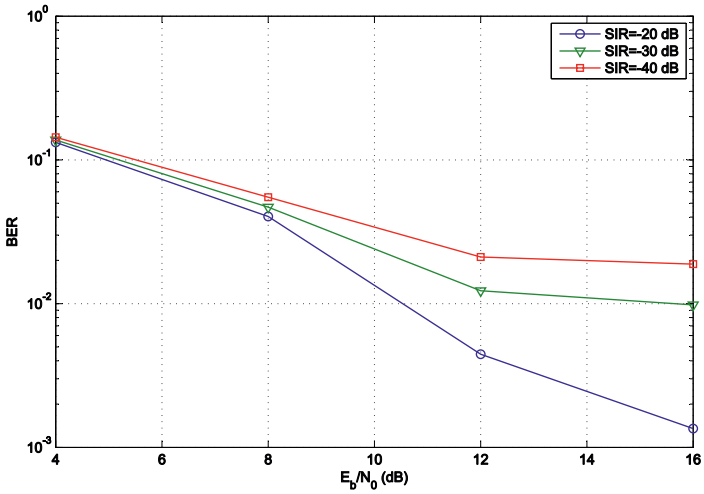

Figure 3.3: Bit error rate (BER) measured at the sensor that deviates from the uniform access scheduling. $\frac{E_b}{N_0}$ is energy per bit to AWGN power ratio, and SIR is Signal to NBI power ratio.

3.6 Conclusion

A transmitting schedule for users/sensors in a multiband/multiuser IR-UWB system is found. The schedule aims to provide a steady state to all the users within the communication system. If we define the steady state as the state where no single sensor can gain smaller BER by changing its transmitting subband for itself, this definition corresponds to Nash equilibrium of a mixed strategic non-cooperative game. Therefore, the multiuser multiband IR-UWB is modeled as n-transmitter jammer game and its mixed strategic Nash equilibrium is found. We prove that the scheduling policy that lets users access each subband with uniform chance is in the Nash equilibrium, and by simulation it is also shown that no single sensor can gain more benefit by deviating from the scheduling policy for itself.

Chapter 4

Robustness via Modulation

4.1 Introduction

This chapter proposes a new modulation that can be used in multiband wireless communication systems to make them robust against narrowband interference. The modulation is able to recover some errors that have occurred due to interference, inherently. The work of this chapter is published in [49].

The rest of the chapter is organized as following. Section 4.2 presents background and motivation for the work presented in this chapter. Section 4.3 describes the new proposed modulation, i.e., pule position and frequency modulation (PPFM). In section 4.4 a receiving algorithm for PPFM is proposed. Section 4.5 presents the results. And section 4.6 concludes this chapter.

4.2 Background and Motivation

For keeping the complexity of a UWB wireless system low, there might be possibilities to lessen the impact of NBI on the performance of the system via modulation techniques. Examples of such approach can be seen in [21] and [16] where they modified transmitted reference ultra wideband (TR-UWB) modulation to deal with NBI. However, a disadvantage of the transmitted reference system is that it dilutes the transmitted power by having to transmitt the reference [25]. Here we introduce a method to mitigate interference based on a new modulation which is simple, works well when NBI signal is strong, and does not dilute the transmitted power. A typical modulation used in UWB is pulse position modulation (PPM) [86, 31]. Based on PPM we propose pulse position and frequency modulation (PPFM) as the new modulation with inherent error correction capabilities. Then, we define a receiving (demodulating) algorithm for PPFM modulated signal that is able to mitigate strong narrow-band interferences. The proposed method is a general technique which can be used in multiband wireless communication systems, and here, as an instance, we use it within a UWB system.

4.3 Pulse Position and Frequency Modulation (PPFM)

Conventional PPM is one of the popular data modulation options in UWB. PPM has different attractive features, among those are power efficiency and opportunity of using non-coherent detection at the receiver [31, 4]. In PPM the position of each pulse within a time frame is decided by the value of a bit to be transmitted while the pulse phase and amplitude remain the same. We can express PPM as:

$$x(t) = p_{tr}(t - \delta d_b), \qquad d_b = \begin{cases} 0 & (b = 0) \\ 1 & (b = 1) \end{cases}, \tag{4.1}$$

where $x(t)$ is the modulated signal to be transmitted, p_{tr} is the pulse shape of the signal, δ is the fixed parameter of PPM that specifies the

amount of shift in position, and d_b gets its value according to the bit, b, to be transmitted [3, 55]. For simplicity reasons we note p_{tr} as p from now on.

Based on PPM we apply a change to get a new data modulation with new features. We modify PPM such that the position and the frequency band of the pulse, both together, are changed depending on the transmitted bit. Analytically, we can represent it as

$$x(t) = p_k(t - \delta d_b), \;\; (d_b, k) = \begin{cases} (0, i) & (b = 0) \\ (1, j) & (b = 1) \end{cases} \; i \neq j, \tag{4.2}$$

where p_k is the pulse shape of the signal in frequency band with center frequency f_k, and k assumes its values from a set, i.e. $\{i, j\}$, depending on the bit value.

Figure 4.1 shows a schematic of pulse position and frequency modulation (PPFM). In PPFM both time and frequency resources are used together.

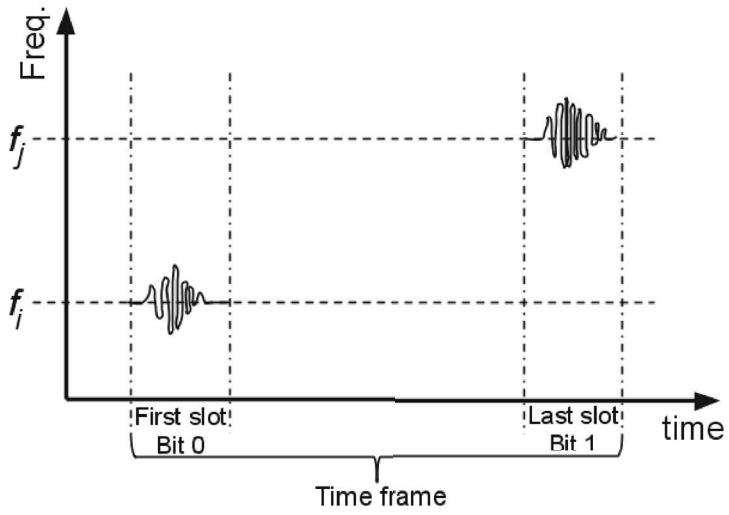

Figure 4.1: Pulse position and frequency modulation (PPFM)

PPFM offers some attractive features, where one of them is that the time

distance between pulse positions, i.e. d_b, can be reduced or even removed depending on the system's criteria. This feature can increase the throughput of the communication link. Another nice feature is that it makes it possible to mitigate strong narrow-band interferences. Following we describe a receiving (demodulating) algorithm that mitigates interferences by use of the inherent property of PPFM.

4.4 Demodulation Algorithm

In this section we describe the receiving algorithm for PPFM modulated signals that mitigates strong NBIs. We assume to have a non-coherent and synchronized receiver. Since the pulse shapes are known to the receiver, we use match filtering to find inhabited energies at available time-frequency positions, and then the algorithm is applied. Let us first define some notations.

$$
\begin{aligned}
B_k &: \text{subband with center freq. } f_k, k = \begin{cases} i & (b=0) \\ j & (b=1) \end{cases} \\
p_k &: \text{pulse i.e. transmitted in } B_k \\
N &: \text{no. of samples of each pulse} \\
A &: \text{pulse energy, } \sum_{l=1}^{N} {p_{kl}}^2 = A \\
s &: \text{time slot no., } s = \begin{cases} 0 & (b=0) \\ 1 & (b=1) \end{cases}
\end{aligned}
$$

$$
\begin{aligned}
Y_{ks} &: \text{observed signal in } B_k \text{ at time slot } s \\
E_{ks} &: \text{observed energy in } B_k \text{ at time slot } s, \\
&\quad E_{ks} = \sum_{l=1}^{N} Y_{ksl} p_{kl} \\
n &: \text{Gaussian noise} \\
\sigma_n^2 &: \text{noise variance}
\end{aligned}
$$

Now let us consider the following cases:

(a) Assume that bit zero, $b = 0$, is transmitted in B_i at the first time slot, $s = 0$, then we have:

$$\begin{aligned} Y_{i0} &= p_i + n, && (4.3)\\ E_{i0} &= \sum_{l=1}^{N} Y_{i0l} p_{il} = \sum_{l=1}^{N} {p_{il}}^2 + \sum_{l=1}^{N} n_l p_{il} && (4.4)\\ &= A + \sum_{l=1}^{N} n_l p_{il}, \\ |E_{i0}| &= |A + \sum_{l=1}^{N} n_l p_{il}| \leq |A| + |\sum_{l=1}^{N} n_l p_{il}| && (4.5)\\ &= |A| + W, \end{aligned}$$

and at the same time in B_i and B_j at the first and the last time slots, $s = 0$ and $s = 1$ respectively, we have:

$$\begin{aligned} E_{i1} &= \sum_{l=1}^{N} n'_l p_{il}, && (4.6)\\ E_{j0} &= \sum_{l=1}^{N} n''_l p_{jl}, && (4.7)\\ E_{j1} &= \sum_{l=1}^{N} n'''_l p_{jl}. && (4.8) \end{aligned}$$

(b) Assume that bit one, $b = 1$, is transmitted in B_j at the last time slot,

$s = 1$, then we have:

$$\begin{aligned} Y_{j_1} &= p_j + n, && (4.9)\\ E_{j_1} &= \sum_{l=1}^{N} Y_{j_1 l} p_{j_l} = \sum_{l=1}^{N} {p_{j_l}}^2 + \sum_{l=1}^{N} n_l p_{j_l} && (4.10)\\ &= A + \sum_{l=1}^{N} n_l p_{j_l}, \\ |E_{j_1}| &= |A + \sum_{l=1}^{N} n_l p_{j_l}| \leq |A| + |\sum_{l=1}^{N} n_l p_{j_l}| && (4.11)\\ &= |A| + W', \end{aligned}$$

and at the same time in B_j and B_i at the first and the last time slots we have:

$$\begin{aligned} E_{j_1} &= \sum_{l=1}^{N} n'_l p_{j_l}, && (4.12)\\ E_{i0} &= \sum_{l=1}^{N} n''_l p_{i_l}, && (4.13)\\ E_{i1} &= \sum_{l=1}^{N} n'''_l p_{i_l}. && (4.14) \end{aligned}$$

Then we apply the following algorithm at the receiver:

1. Check if following equations are satisfied

$$|E_{i0}| \leq |A| + W + \theta \quad (4.15)$$
$$|E_{j_1}| \leq |A| + W' + \theta \quad (4.16)$$

   where θ is an arbitrary threshold.

2. If step 1 is satisfied go to step 3, otherwise go to step 4.

3. Received bit is found by processing the differential energy such as

$$E_{diff} = E_{i0} - E_{j_1} = \sum_{l=1}^{N} Y_{i0_l} p_{i_l} - \sum_{l=1}^{N} Y_{j_1 l} p_{j_l}, \quad (4.17)$$

$$\tilde{b} = \begin{cases} 0 & E_{diff} \geq 0 \\ 1 & E_{diff} < 0 \end{cases}, \tag{4.18}$$

where $\tilde{b}$ is the received bit.
End.

4. Find out which equation in step one is not satisfied.
   If Equation (4.15) is not satisfied go to step 5.
   If Equation (4.16) is not satisfied go to step 6.

5. If

$$\begin{aligned} |E_{j_1}| &\leq W'' + \theta' \\ W'' &= {\sigma_n}^2 \end{aligned} \tag{4.19}$$

   is satisfied it means that no pulse is sent in this band at this time slot, so we conclude that $b = 0$ is transmitted which is corrupted by some strong interference, so $\tilde{b} = 0$.
   End.

   Else we conclude that $\tilde{b} = 1$ is transmitted.
   End.

6. If

$$\begin{aligned} |E_{i0}| &\leq W'' + \theta' \\ W'' &= {\sigma_n}^2 \end{aligned} \tag{4.20}$$

   is satisfied it means that no pulse is sent in this band at this time slot, so we conclude that $b = 1$ is transmitted which is corrupted by some strong interference, so $\tilde{b} = 1$.
   End.

   Else we conclude that $\tilde{b} = 0$ is transmitted.
   End.

With this algorithm the receiver can recover the signal from errors that have occurred due to strong interferences. In next section we simulate a system with the proposed modulation and demodulation algorithm.

4.5 Results

The proposed modulation is simulated with the following system model and the simulation results are given afterwards.

4.5.1 System Model

The proposed modulation and algorithm can be applied generally in multiband wireless communications. Here, we explain an application in multiband UWB wireless communication, while we propose a new multiband UWB scheme.

We consider impulse radio (IR) technique for UWB communications. With a multiband signaling scheme the UWB spectrum is divided into 15 frequency bands. One of the frequency bands is reserved for controlling messages and the other bands are used for data transmission. Figure 4.2 shows the frequency bands and bit allocation. As it is shown, frequency bands are divided into two groups. One group is allocated to bit value 0, i.e., only when $b = 0$ a pulse is transmitted through one of the bands in this group. The other group is allocated to bit value 1. We also introduce a set of frequency band pairs such as $\{(B_1, B_8), (B_2, B_9), \cdots, (B_7, B_{14})\}$. We assume to have maximum distance between two center frequencies of each frequency band within each pair. Depending on the design this distance can be same for all pairs, which is the case here. The reason behind this pairing design is to decrease the probability of both bands within each pair to be interfered by a single narrow-band interference. This pairing also helps to obtain better usage of frequency diversity.

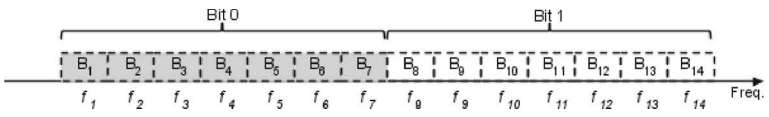

Figure 4.2: Frequency bands allocation.

Data bits at the transmitter are packed in strings which have a size equal to the number of pairs, i.e., 7 bits here. When transmitter starts to send a string, the first data bit is sent through the first pair of bands, the second bit through of the second pair of bands, and similarly to the last bit of the string which is sent through the last pair of bands, i.e., the seventh pair here. To make it more clear let us give an example. Assume that we have this string $\{0, 0, 1, 0, 1, 1, 0\}$ to transmit, starting on the left. The transmission takes the following pattern:

bit	a pulse is sent via	*no* pulse is sent via
0	B_1	B_8
0	B_2	B_9
1	B_{10}	B_3
0	B_4	B_{11}
1	B_{12}	B_5
1	B_{13}	B_6
0	B_7	B_{14}

At the receiver, both time slots within each frame for both frequency bands are observed, and the proposed algorithm is applied to receive the transmitted bits. The receiver is non-coherent and assumed to be synchronized.

For each of the 14 frequency bands a pulse shape is designed according to the algorithm defined in [58]. The pulse shapes are spectrally efficient, that means the pulse's spectrum nearly fits the specified frequency spectrum. A summary of the pulse design method is given in Appendix A.

We assume additive white Gaussian noise (AWGN) channel that is interfered with narrow-band interference. NBI can be of any sort of narrow-band wireless communication system that works within the UWB frequency band, 3.1-10.6 GHz. For the simulation we assume that NBI source is IEEE802.11 services with frequency range of 5.15-5.35 GHz. Note that the choice of narrow-band interference does not affect the performance of the system and the simulation results, since the proposed system is a blind system that works irrespective of the position of NBI [50, 51].

4.5.2 Simulation Results

Two systems, one with PPM and one with PPFM are simulated in order to compare the results and find the benefits of the new modulation, namely PPFM. Figure 4.3 shows a simple block diagram of the simulated system model.

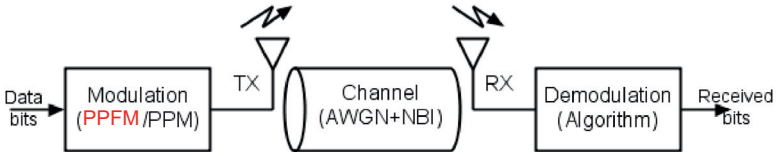

Figure 4.3: Simple block diagram of the system model.

Figure 4.4 shows the simulation result of the system with PPM for the explained model. We can see that for signal to interference ratio (SIR) values less than or equal to 0dB, the performance becomes very poor. The reason is that when NBI interferes a frequency band, both time slots of the PPM frame are affected by the NBI and it is not possible to find out in which time slot a pulse is sent. Therefore, NBI, with its high power, jams the receiver and the performance degrades.

Figure 4.5 shows the simulation result of the system with PPFM for the explained model. It can be seen that the performance has been improved compared to system with PPM. If we consider the bit error rate (BER) at the energy per bit to noise ratio (E_b/N_0) equal to 12dB, it is seen that the performance is much better for almost all SIR values except for SIR values for -40dB and -50dB. The reason is explained later. Thus, as expected PPFM helps to mitigate strong NBI. This robustness against NBI relies on the nature of PPFM and the demodulation algorithm. As was explained previously, frequency shift in addition to time shift in the modulation makes it possible to correct some errors occurred by NBI with use of a proper multiband scheme and the receiving algorithm.
The reason that the performance for SIR values -40dB and -50dB is not as good as it is expected and it is worse than the performance for lower

SIR values is that in this range of SIR the receiving algorithm experiences much difficulty for comparing observed energies. However, even in this range the performance is slightly better than the performance for PPM.

Simulation results are promising and show that the proposed technique on PPFM is able to mitigate strong NBI. We must also mention that the whole system is blind regarding NBI. It means that this system is robust against unknown NBI and information about center frequency of NBI is not required.

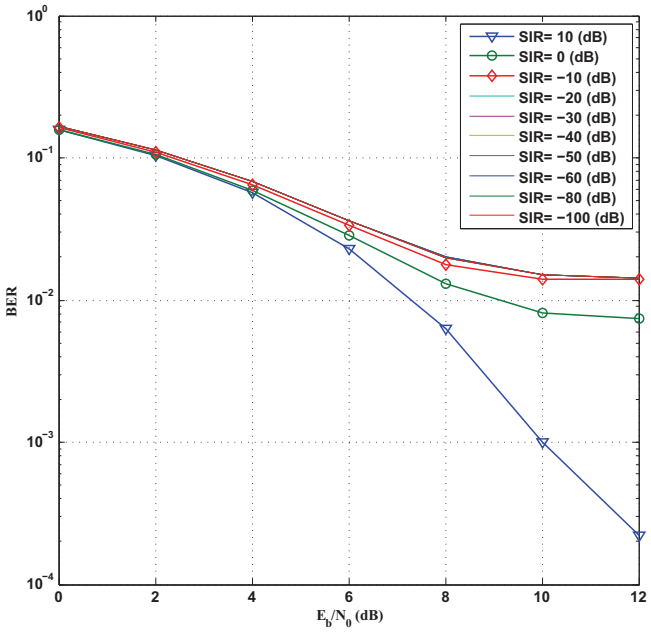

Figure 4.4: Performance with pulse position modulation (PPM) and the explained UWB system. BER: Bit error rate. $\frac{E_b}{N_0}$: Energy per bit to noise ratio. SIR: Signal to interference ratio. For SIR values from -10 to -100 the curves are lied on each other.

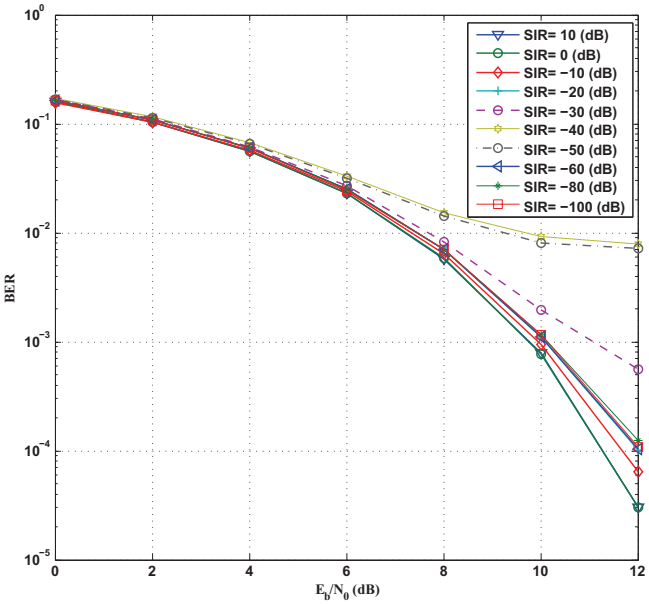

Figure 4.5: Performance with pulse position and frequency modulation (PPFM) and the explained UWB system. BER: Bit error rate. $\frac{E_b}{N_0}$: Energy per bit to noise ratio. SIR: Signal to interference ratio.

4.6 Conclusion

In this chapter a new pulse position and frequency modulation (PPFM) based on pulse position modulation (PPM) has been proposed to mitigate strong narrow band interferences (NBIs) in multiband wireless communication systems. Also we have proposed a receiving (demodulation) algorithm for PPFM, which is able to mitigate NBI. PPFM and the proposed demodulating algorithm make it possible to correct some errors which occur due to unknown NBI without using any error correction coding.

One possible application of the proposed technique can be found in multiband ultra wideband (UWB) communication systems. We describe a new

multiband UWB scheme to evaulate the proposed algorithm as a proof of concept. A comparision between PPFM with conventional PPM and the proposed scheme has been performed. The simulation results show that PPFM with differential receiving algorithm mitigates strong NBI and performs better than the conventional system with PPM. Furthermore the proposed method is a good candidate for multiuser scenarios utilizing the degrees of freedom in terms of time and frequency.

Chapter 5

Feedback in UWB Wireless Sensors Network with Compressed Sensing

5.1 Introduction

Up till now, through previous chapters, we have only discussed robustness techniques for a blind system that has no information about the communication channel and receives no feedback. However, a way to make the system more robust against interferences is to provide feedback and information about its proximity. If some or all sensors in the network are able to estimate the spectrum of the communication channels, we can apply techniques from cognitive radio (CR). There is a clear connection between players in CR scenario and UWB sensors network. That is, secondary users (cognitive radios) in a CR scenario are similar to sensors (transmitters) in UWB sensors network, and primary users in CR scenario are similar to narrowband interferences in UWB sensors network. CR is further explained in this chapter. But applying CR technique to UWB sensors network means that sensor nodes need to sample a wideband spectrum and it can be a very cumbersome task for a wireless node. Therefore we intend to apply a technique that makes this task simpler to

some extent. The work of this chapter is published in [52] and [28].

The rest of this chapter is organized as following. Section 5.2 presents a background on the work. Section 5.3 formulates the problem. Section 5.4 explains the proposed sensing technique based on combined compressed sensing and distribution discontinuities detection. Section 5.5 is dedicated to simulation results, and section 5.6 concludes this chapter.

5.2 Background

The increasing demand for spectrum from various wireless devices and networks emerges the technical society to use the radio spectrum more efficiently. Measurements lead by the FCC (Federal Communication Commission) in the USA have shown that in some regions and/or at some day intervals up to 70 percent of the statically allocated spectrum is left idle [23]. Facing this inefficient usage of spectrum, the FCC recommends deploying unlicensed users in the wireless networks. These unlicensed users, also called secondary user (SU), are allowed to use those idle wireless resources only when the licensed users, also called primary user (PU), are not using them so they do not interfere with their transmissions. In order to make such a concept of spectrum sharing feasible, SUs are cognitive radios (CRs) deployed in the primary networks. CR as introduced by Joseph Mitola [35] is a self aware and intelligent device that can adapt itself to the wireless environment changes by first detecting them, and then adapting its radio parameters to the new opportunities. Detection of spectrum holes is of the first steps of implementing a cognitive radio system. Different statistical approaches already exist. The easiest to implement and the reference system in terms of complexity is the energy detector (ED) [76]. Nevertheless, the ED is highly sensitive to noise and does not perform well in low signal to noise ratios (SNR). Other advanced techniques based on signal modulations and exploiting some of the transmitted signals inner features were also developed [63]. For instance, the cyclostationary features detector (CFD) exploits the built-in cyclic properties of the PU received signal. The CFD has a great robustness to noise compared to ED but its high complexity is still a consequent drawback. Other tech-

niques that were developed by researchers at Eurécom Institute are based on model selection tools and entropy investigation [81, 82, 33].

An important complexity factor in sensing wideband spectrum by cognitive radios is the required sampling rate at CR nodes that tends to be very high. Also, applying the mechanism of narrowband detector for wideband spectrum sensing is inflexible and slow. Therefore, efficient wideband sensing techniques are highly demanded to increase the sensing agility [60].

Compressed sensing/compressive sampling (CS) has been considered as a promising technique to improve and implement cognitive radio (CR) systems. In CS a signal with a sparse representation in some basis can be recovered from a small set of nonadaptive linear measurements [19]. Typically the wireless signal in open access networks is sparse in the frequency domain since depending on location and at some times the percentage of spectrum occupancy is low due to the idle radios [73, 34]. Figure 5.1 shows an example of signal sparsity. A sensing matrix takes few measurements of the signal, and the original signal can be reconstructed from the incomplete and contaminated observations approximately and sometimes exactly by solving a convex optimization problem [9, 6]. In [10] and [11] conditions on this sensing matrix are introduced which are sufficient in order to recover the original signal stably. Remarkably, a random matrix fulfills the conditions with high probability and performs an effective sensing [8, 19].

Apart from reconstructing the original signal, detection is more interesting in the context of cognitive radio. Generally, for detection purposes it is not necessary to reconstruct the original signal, but only an estimate of the relevant sufficient statistics for the problem at hand is enough. This leads to less measurements and lower computational complexity [22]. We are interested in skipping the estimation of the original signal and directly use the measurements for detection purpose, and thus reduce the complexity of the system as much as possible.

In [73] a wavelet-based detection approach using CS to identify the spec-

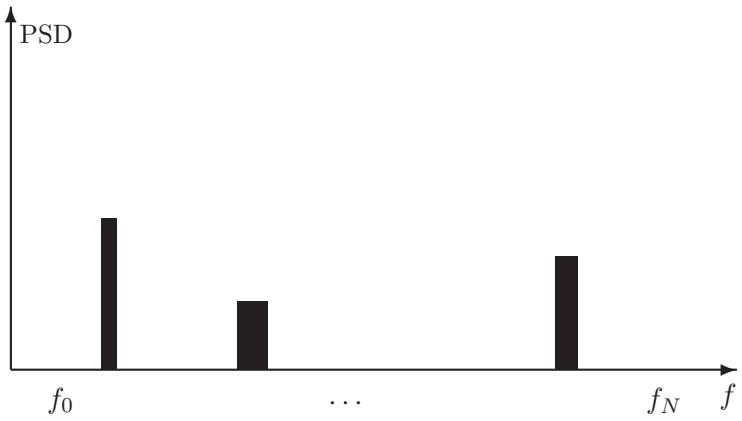

Figure 5.1: An example of power spectral density vs. the frequency of a spectrally sparse wideband signal. PSD stands for power spectral density and f stands for frequency.

trum holes is introduced. To find the frequency band boundaries they derive a convex optimization formulation that the solution gives the band boundaries of the spectrum without requiring to reconstruct the original signal.

In this chapter we develop a combined compressive sampling and distribution discontinuities detection technique based on algebraic method for the sensing task of identifying the spectrum holes. The proposed algebraic detector is a linear detector and we would like to feed the algorithm directly with the compressed measurements. For this purpose we find a proper sensing matrix that gives the possibility of feeding the algebraic detector directly with the measurements.

Furthermore, it is generally a requirement to have cooperative sensing to make hidden nodes detectable for CR nodes. It means several CR nodes sense the spectrum cooperatively to detect PUs and available holes. In such scenarios, the amount of data processing at each CR node, in both centralized and decentralized schemes, and the amount of data exchange

between CR nodes and the fusion center in the centralized scheme are important factors in complexity and power consumption of the system. In this regard, we develop a centralized implementation of collaborative compressed sensing of wideband spectrum for cognitive radios that is combined with distribution discontinuities detection technique.

5.3 Problem Formulation

Let us consider a discrete representation of the received signal given by:

$$x(n) = A_n s(n) + e(n) \tag{5.1}$$

where A_n is modeling the channel, $s(n)$ represents the discrete signal, that is $s(t)$ sampled at Nyquist rate, and $e(n) \sim \mathcal{N}(0, \sigma^2 I_n)$ is i.i.d. Gaussian noise where I_n is an identity matrix of size n.

We would like to distinguish between two classified hypothesis $\mathcal{H}_0$ and $\mathcal{H}_1$:

$$\mathcal{H}_0 \quad : \quad x(n) = e(n) \tag{5.2}$$
$$\mathcal{H}_1 \quad : \quad x(n) = A_n s(n) + e(n) \tag{5.3}$$

where $\mathcal{H}_0$ means that the sensed frequency band is white containing only noise and $\mathcal{H}_1$ means that the sensed frequency band is occupied with a signal corrupted by noise. The key parameter of all spectrum sensing algorithms are the false alarm probability P_F and the detection probability P_D. P_F is the probability to determine a frequency band as occupied while it is free, thus P_F should be kept as small as possible.

$$P_F = P(\mathcal{H}_1|\mathcal{H}_0) = P(\text{a signal (user) is present}|\mathcal{H}_0) \tag{5.4}$$

P_D is the probability to determine a frequency band as occupied when there exists a signal, thus P_D should be kept as large as possible.

$$P_D = 1 - P_M = \tag{5.5}$$
$$1 - P(\mathcal{H}_0|\mathcal{H}_1) = 1 - P(\text{no signal (user) is present}|\mathcal{H}_1)$$

where P_M denote the probability of missed detection. To design the optimal detector based on the Neyman-Pearson criterion, we try to maximize the overall P_D under a given overall P_F.

In order to infer on the nature of the received signal, we calculate a threshold for each of the detectors. The decision threshold is determined using the required probability of false alarm P_F given by 5.4. The threshold Th for a given P_F is determined by solving the equation:

$$P_F = P(\text{a signal is present}|\mathcal{H}_0)) = 1 - F_{\mathcal{H}_0}(Th) \tag{5.6}$$

where $F_{\mathcal{H}_0}$ denote the cumulative distribution function (CDF) under $\mathcal{H}_0$.

The algebraic approach is able to detect the signal distribution discontinuities and find their positions in the spectrum, having the complete signal (Nyquist rate samples) as input to the detector. The problem is that sampling a wideband signal with Nyquist rate is constrained due to the reasons highlighted in Section 5.1. For detecting with smaller sampling rate, relative to Nyquist rate, compressed sensing technique is used. In this case, considering the sparseness of the signal, the received signal is observed compressively as:

$$y = \Phi x + e \tag{5.7}$$

where $y \in \mathbb{R}^M$ is the compressed measurements, Φ is the sensing matrix, $x \in \mathbb{R}^N$ is the received signal like $A_n s(n)$ as in (5.1), e is the additive noise, and $M \ll N$. It is shown that with some conditions on Φ it is possible to recover x accurately based on y [9].

It is desirable to use the compressed samples directly for frequency holes detection and without recovering the signal itself. Since the algebraic detection of distribution discontinuities is a linear approach, a proper sensing matrix is required that makes it possible to use the compressed samples as input to the linear detector. In following section we discuss compressed sensing and selection of such sensing matrix.

5.4 Combined Compressed Sensing and Distribution Discontinuities Detection

5.4.1 Compressed Sensing

Let $x \in \mathbb{R}^N$ be a signal with expansion in an orthonormal basis Ψ as

$$x[n] = \sum_{j=0}^{N-1} \alpha_j \psi_j[n], \quad n = 0, \cdots, N-1 \tag{5.8}$$

where Ψ is the $N \times N$ matrix with the waveforms ψ_j as rows. To use convenient matrix notations we can write the decomposition as $x = \Psi\alpha$ or equivalently, $\alpha = \Psi^* x$ where Ψ^* denotes conjugate transpose of Ψ. A signal x is sparse in the Ψ basis if the coefficient sequence α is supported on a small set. We say that a vector α is S-sparse if its support $\{j : \alpha_j \neq 0\}$ is of cardinality less or equal to S [6]. Consider that we would like to recover all the N coefficients of x, vector α, from measurements y about x of the form

$$y_m = \langle x, \phi_m \rangle = \sum_{n=0}^{N-1} \phi_{mn} x[n], m = 0, \cdots, M-1 \tag{5.9}$$

or

$$y = \Phi x = \Phi\Psi\alpha = \Theta\alpha \tag{5.10}$$

where we are interested in the case that $M \ll N$, and the rows of the $M \times N$ sensing matrix Φ are incoherent with the columns of Ψ. Then it is shown that signal x can accurately and sometimes exactly be recovered, considering that the recovered signal $x^\star$ is given by $x^\star = \Psi\alpha^\star$, and $\alpha^\star$ is the solution to the convex optimization program

$$\min_{\tilde{\alpha} \in \mathbb{R}^N} ||\tilde{\alpha}||_{l_1} \text{ subject to } \Phi\Psi\tilde{\alpha} = \Theta\tilde{\alpha} = y \tag{5.11}$$

where $||\tilde{\alpha}||_{l_1} := \sum_{j=1}^{N} |\tilde{\alpha}_j|$. The compressed sensing (CS) theory states that there exists a measuring factor $c > 1$ such that only $M := cS$ incoherent measurements y are needed to recover x with high probability.

We also have to mention that except l_1-minimization solution other methods such as greedy algorithms in [74] exist for recovering the sparse signal [8, 6, 20, 7, 9, 22].

In case of noisy measurements, i.e., $y = \Phi x + e$, where e is noise with $||e||_{l_2} \leq \epsilon$, [9] shows that solution to

$$\min_{\tilde{\alpha} \in \mathbb{R}^N} ||\tilde{\alpha}||_{l_1} \text{ subject to } ||\Theta\tilde{\alpha} - y||_{l_2} \leq \epsilon \tag{5.12}$$

recovers the sparse signal with an error at most proportional to the noise level. Also, [9] discusses the conditions for stable recovery from noisy measurements.

We are interested in detection of spectrum holes by using algebraic approach *directly* from the compressed measurements without reconstructing the original signal itself. For this reason we must find out the appropriate sensing matrix according to the detection technique. The proposed detection technique is a linear algebraic algorithm. This technique uses the Fourier transform of the observed signal to detect the occupied frequency bands in the observed spectrum. Therefore the compressed measurements of the observed signal must keep the linearity and properties of the original signal in order to apply the detection algorithm successfully on the compressed measurements. To find the sensing matrix we start by looking at the Discrete Fourier transform of the signal $x \in \mathbb{R}^N$.

$$X_l = \sum_{n=0}^{N-1} x[n] \exp(-\omega l n), l = 0, \cdots, N-1, \tag{5.13}$$

where $\omega = \frac{2\pi i}{N}$ and i is the imaginary unit. The Fourier transform of the measured signal is

$$Y_k = \sum_{m=0}^{M-1} y[m] \exp(-\omega k m), k = 0, \cdots, M-1. \tag{5.14}$$

From 5.10 we replace $y[m]$ and we have

$$Y_k = \sum_{m=0}^{M-1} (\sum_{n=0}^{N-1} \phi_{mn} x[n]) \exp(-\omega k m), k = 0, \cdots, M-1, \tag{5.15}$$

where ϕ_{mn} denotes the element of Φ at the cross of row m and column n. Then from the linearity properties we have

$$Y_k = \sum_{n=0}^{N-1} \sum_{m=0}^{M-1} \phi_n[m] \exp(-\omega k m) x[n], k = 0, \cdots, M-1, \tag{5.16}$$

where $\phi_n[m]$ denotes the m^{th} element of the n^{th} column vector of Φ, ϕ_n, and we see that

$$\sum_{m=0}^{M-1} \phi_n[m] \exp(-\omega k m) = \hat{\Phi}_{n_k}, k = 0, \cdots, M-1, \tag{5.17}$$

that is the Fourier transform of the n^{th} column vector of Φ, $\hat{\Phi}_n$. Then from 5.16 and 5.17

$$Y_k = \sum_{n=0}^{N-1} \hat{\Phi}_{n_k} x[n], k = 0, \cdots, M-1. \tag{5.18}$$

And, as we said, in order to feed the detection algorithm directly by the compressed measurements we seek that

$$Y_k(\omega) = a X_l(\omega), k \in \{0, \cdots, M-1\}, l \in \{0, \cdots, N-1\}, \tag{5.19}$$

where $a > 0$ is a constant. From 5.18 and to satisfy 5.19 we find that

$$\hat{\Phi}_{n_k} = a \exp(-\omega z n), z \in \{1, \cdots, N\}, k = 0, \cdots, M-1, \tag{5.20}$$

and therefore from inverse Fourier transform we have

$$\phi_n = a\delta(n - z), z \in \{1, \cdots, N\}, \tag{5.21}$$

which means that any row vector of the sensing matrix is a Dirac function, that is, only one column of each row is nonzero.
Now that the general format of the sensing matrix is clear, we should find a way to generate it. The Φ^T matrix can be generated by randomly selecting M columns of an identity matrix I_N. Φ is given by the transpose of Φ^T, and we define $a = 1$ to make sure that the columns of the sensing

matrix are unit-normed. So the sensing matrix Φ that we obtained has a form like this

$$\Phi \approx \begin{bmatrix} 0 & 1 & 0 & \cdots & 0 & 0 & 0 & 0 \\ \vdots & \vdots & \vdots & \vdots & \vdots & \vdots & \vdots & \vdots \\ 0 & 0 & 0 & \cdots & 0 & 0 & 0 & 1 \\ \vdots & \vdots & \vdots & \vdots & \vdots & \vdots & \vdots & \vdots \\ 0 & 0 & 0 & \cdots & 0 & 1 & 0 & 0 \end{bmatrix}_{M \times N} . \tag{5.22}$$

This form of sensing matrix gives us the opportunity to use the compressed measurements directly as input to the algebraic detection algorithm and thus avoiding the computation complexity of reconstructing the original signal. Next the algebraic detection technique with compressed measurements as the input to the algorithm is explained.

5.4.2 Algebraic Detection Based on Compressive Sampling

The algebraic detection (AD) is a new approach based on advanced differential algebra and operational calculus. In this method, the primary user's presence is rather casted as a change point detection in its transmission spectrum [29]. In this approach, the mathematical representation of the spectrum of the compressed measurements, i.e., the observed signal Y_n in frequency domain, is assumed to be a piecewise P^{th} polynomial signal expressed as following:

$$Y_n = \sum_{k=1}^{K} \mathcal{Y}_k[n_{k-1}, n_k](f) p_k(n - n_{k-1}) + E_n, \tag{5.23}$$

where $\mathcal{Y}_k[n_{k-1}, n_k]$ is the characteristic function, p_k is a polynomial series of order P, E_n is the additive corrupting noise, K is the number of subbands defined in the frequency range of observation interest, and $n = \frac{f}{f_s}$ is the normalized frequency, where f_s is the sampling frequency and f is the signal frequency.
Let us define the clean version of the received signal S_n as:

$$S_n = \sum_{k=1}^{K} \mathcal{Y}_k[n_{k-1}, n_k](f) p_k(n - n_{k-1}) \tag{5.24}$$

And let b, the frequency band, such that one and only one change point occurs in the interval $I_b = [n_{k-1}, n_k] = [\nu, \nu + b]$, $\nu \geq 0$. Denoting $S_\nu(n) = S(n + \nu)$, $n \in [0, b]$ as the restriction of the signal in the interval I_b and redefine the change point n_ν relatively to I_b such as:

$$\begin{cases} n_\nu = 0 & \text{if } S_\nu \text{ is continuous} \\ 0 < n_\nu \leq b & \text{otherwise} \end{cases} \tag{5.25}$$

Then, the primary user presence on a sensed sub-band is equivalent to find $0 < n_\nu \leq b$ on that band. The AD gives the opportunity to build a whole family of spectrum sensing detectors, depending on a given model order P. Depending on this model order, we can show that performance of the AD is increasing as the order P increases.

The proposed algorithm is implemented as a filter bank composed of P filters in parallel. The impulse response of each filter is:

$$h_{k+1,n} = \begin{cases} \frac{(n^l(b-n)^{P+k})^{(k)}}{(l-1)!}, 0 < n < b \\ 0, \quad \text{otherwise} \end{cases} \tag{5.26}$$

where $k \in [0 \cdots P-1]$ and l is chosen such that $l > 2 \times P$. The proposed expression of $h_{k+1,n}$, $k \in [0 \cdots P-1]$ is determined by modeling the spectrum with a piecewise regular signal in frequency domain and casting the problem of spectrum sensing as a change point detection in the primary user transmission [29]. Finally, in each detected interval $[n_{\nu_i}, n_{\nu_{i+1}}]$, we compute the following equation:

$$\lambda_{k+1} = \sum_{m=n_{\nu_i}}^{n_{\nu_{i+1}}} W_m h_{k+1,m} X_m, \tag{5.27}$$

where M is the number of samples of the observed signal, and W_m is the weight for numeric integration defined by:

$$\begin{cases} W_0 = W_M = 0.5 \\ W_m = 1 \quad \text{otherwise} \end{cases} \tag{5.28}$$

In order to infer whether the primary user is present in its interval, a decision function is computed as following:

$$Df = \| \prod_{k=0}^{P} \lambda_{k+1}(n_\nu) \| \tag{5.29}$$

The decision is made by comparing the threshold Th to the mean value of the decision function over the detected intervals.

5.4.3 Centralized Collaborative Compressed Sensing

In a centralized collaborative implementation of cognitive radios, each radio communicates with the fusion center through a control channel. Any of the radios individually performs compressive sensing and sends its observation to the fusion center.

The compressed observations from each radio is processed separately at the fusion center with an algebraic approach. In the collaborative sensing the final decision is made by applying a rule on the decisions from all the radios for each detected interval. Different rules maybe used, and here we choose the averaging rule. Let us denote the detection results from collaboration by $\mathcal{D}$. Decision function from each radio ρ on each interval $[\nu_i, \nu_{i+1}]$ is denoted by Df_{ρ,ν_i}. Then we have:

$$\mathcal{D}_\nu = \frac{1}{Rs} \sum_{\rho=1}^{Rs} Df_{\rho,\nu_i}, \tag{5.30}$$

where Rs is the number of collaborative radios, and Df is given by equation (5.29). Thus, the final decision is made by comparing $\mathcal{D}$ to the threshold Th over the detected subbands.

5.5 Simulation Results

In this section we investigate the performance of the proposed algorithm in comparison with the energy detector (ED). First we consider a frequency

band in the range of $[50, 250]$MHz, in order to compare the compressive sensing using the algebraic method and the wavelet approach introduced in [72]. The signal is fully described in [72]. During the observed burst of transmissions in the network there are 6 bands with frequency boundaries at $n_{\nu_i,}|_{i=0}^{6} = [50, 120, 170, 200, 220, 224, 250]$ MHz.

Comparing with the wavelet approach, in the algebraic detection technique change points are detected in a single action, while in the wavelets approach, many detections have to be conducted and fused to make a final decision. Figure 5.2 shows the algebraic detection performance on this signal.

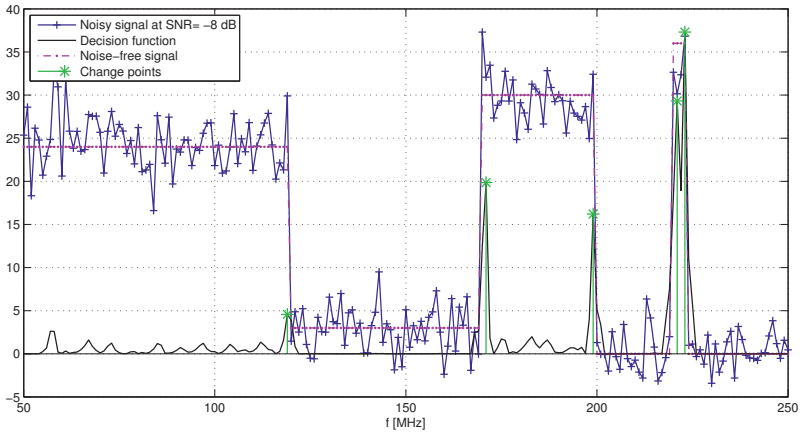

Figure 5.2: Edge detection using the algebraic technique. The signal in red is the original signal, the one in blue is the noisy observation with SNR=-8dB. The black signal is the computed decision function and the green stars are the detected change points.

Now, comparing the proposed compressed sensing algorithm to the reference algorithm, let us give some key notes on the ED. ED is the most common method for spectrum sensing because of its non-coherency and low complexity. The energy detector measures the received energy during a finite time interval and compares it to a predetermined threshold. That

is, the test statistic of the energy detector is:

$$\sum_{m=1}^{M} \| y_m \|^2, \tag{5.31}$$

where M is the number of samples of the received signal y.

Traditional ED can be simply implemented as a spectrum analyzer. A threshold used for primary user detection is highly susceptible to unknown or changing noise levels. Even if the threshold would be set adaptively, presence of any in-band interference would confuse the energy detector.

Since the complexity of sensing algorithms is a major concern in implementation and ED is well known for its simplicity, we choose ED as the comparison reference. Denoting N the number of Nyquist samples of the observed signal y and P the model order of AD, we show that the complexity of AD is PN and the complexity of ED is N. From these results, we clearly see that the exploited sensing algorithm has a comparable complexity to the energy detector. For the proposed AD based compressed sensing algorithm, the complexity is equal to: $P\frac{M}{N}N = PM$, where M is the number of compressed measurements of the received signal and $M \ll N$. Table 5.1 summarizes the complexity of each detector.

Sensing technique	Complexity
Energy detector	N
Algebraic detector	PN
Combined compressive sampling and distribution discontinuities detection	PM

Table 5.1: Complexity comparison among the three sensing techniques; $M \ll N$.

In order to achieve realistic and well founded simulations, digital video broadcasting-terrestrial (DVB-T) signals are used as the signals to be sensed. This choice can be justified by the fact that almost all licensed

primary networks are DVB-T and secondary users are CR deployed in these networks. Here DVB-T signals are of 2k-mode type, where 2k-mode defines the number of OFDM carriers, in this case 1075, and they are approximately 4KHz apart [64]. The signal parameters are given in Table 5.3.The value of the threshold Th is calculated at $P_F = 0.05$ through a Monte Carlo simulation.

Bandwidth	8MHz
Mode	2K
Guard interval	1/4
Channel models	AWGN
Flat fading	Single path
Sensing time	1.25ms

Table 5.2: The transmitted DVB-T primary user signal parameters

Figure 5.3 shows the performance of the following simulated detectors: energy detector (ED), first order algebraic detector (AD_1), AD_1 with compression rate of $M/N = 20\%, 30\%, 40\%$ and 50% and a second order algebraic detector (AD_2) with $M/N = 50\%$. We note that ED, AD_1 and $AD_2^{50\%}$ all have the same complexity and Figure 5.3 shows that $AL_2^{50\%}$ have a much better performance than ED and at low SNRs it is outperforming AD_1.

Another key metric in the sensing problems is the receiver operating characteristics (ROC) curve which helps giving an idea about the reliability of the proposed technique. For instance we plot the ROC curve at $SNR = -25dB$ for ED, AD_1 and $AL_2^{50\%}$.

Figure 5.4 shows how reliable the compressed sensing technique is, as the detector operates at high probability of detection under a low false alarm rate.

Then we investigate the performance of the proposed collaborative compressed sensing comparing to the energy detector (ED). Consider groups

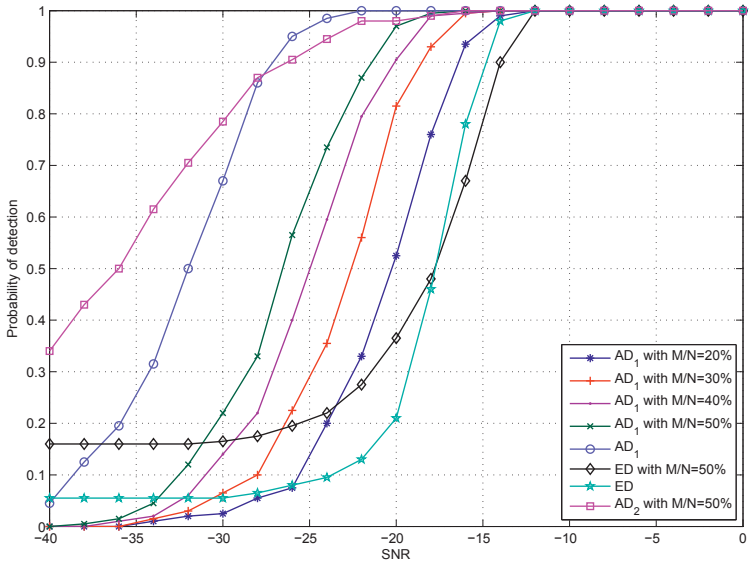

Figure 5.3: P_D vs. SNR at P_F=0.05; AD$_P$:Algebraic detector of order P; ED: Energy detector; $\frac{M}{N}$:Compression ratio.

of collaborative radios with size of $1, 5, 10$, and 20 radios. Each radio communicates with the fusion center through a control channel. We assume that the radio channel between primary users and cognitive radios has a flat fading with a Rayleigh distribution and shadowing effect. Cognitive radios can either use a same sensing matrix or each radio can have a different sensing matrix from other radios. Here, we assume that radios use different sensing matrices from each other that are made randomly in a way that was explained earlier.

Again in order to achieve realistic and well founded simulations, DVB-T signals based on DVB-T 2K recommendations are used as the signals to be sensed. The signal and channel parameters are given in Table 5.3. The value of the threshold Th is calculated at $P_F = 0.05$ through a Monte Carlo simulation.

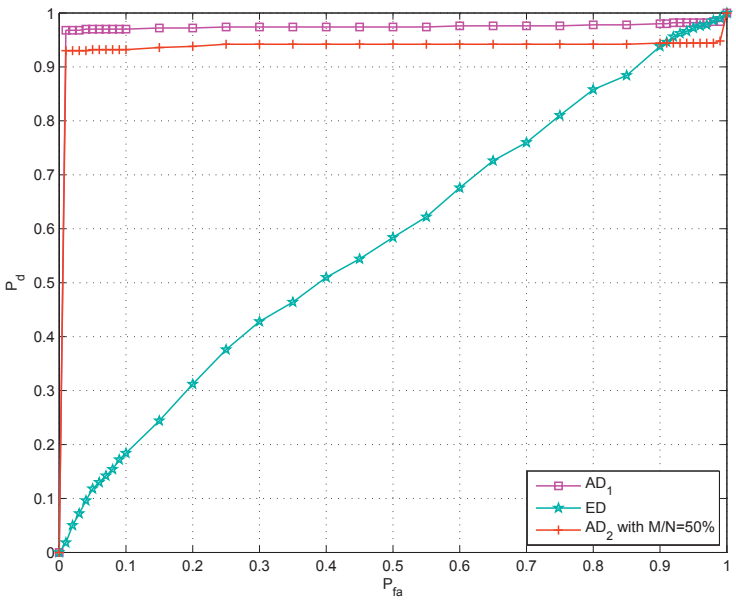

Figure 5.4: ROC curve at SNR=$-25dB$; AD_P :Algebraic detector of order P; ED: Energy detector; $\frac{M}{N}$:Compression ratio.

Bandwidth	8MHz
Mode	2K
Guard interval	1/4
Channel models	AWGN
Flat fading	Multipath
Channel gains	[-10,0]dB
Sensing time	1.25ms

Table 5.3: The transmitted DVB-T primary user signal and channel parameters

For each group size, compressed collaborative detection with different com-

pression ratios, $\frac{M}{N} = \{10\%, 20\%, 30\%\}$, is simulated and compared to the ED detector with single radio and no compression. Collaborative ED is not simulated due to timing issues and since the comparison is still valid with single radio because, as will be seen, performance of a single radio with compressed sensing for compression ratios of about 20% and higher is better than single ED with no compression. So, we expect that cooperative compressed sensing also ourperforms cooperative ED, intuitively.

Figure 5.5 shows the performance of the energy detector (ED) with no compression and a first order algebraic detector AD_1 with different compression ratios for collaborative groups of size $1, 5, 10$ and 20 radios.

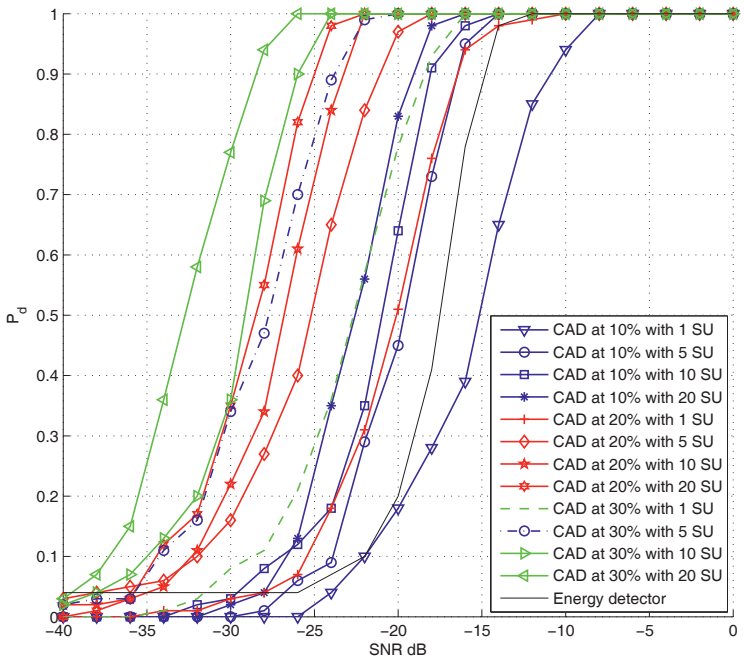

Figure 5.5: Probability of detection, P_D, vs. SNR at $P_F = 0.05$. CAD: Compressed sensing with Algebraic detection of order $P = 1$. SU: secondary users/collaborative radios.

a

We note that performance of a single radio with compression ratio of 10% is not as good as performance of ED with single radio and no compression. And for the rest of examples the performance is better. This is where the complexity of the compressed sensing, i.e., $\frac{M}{N}$, is much lower than ED, i.e., N. Collaboration among radios greatly improves the detection performance. Also, we note that when the number of collaborations increases the compression ratio at each radio can be decreased in order to achieve a specific probability of detection P_D. Figure 5.6 shows the probability of detection that is achievable by different number of collaborative radios for a compressed sensing ratio of $\frac{M}{N} = 10\%$ at SNR$=-20dB$ and $P_F = 0.05$.

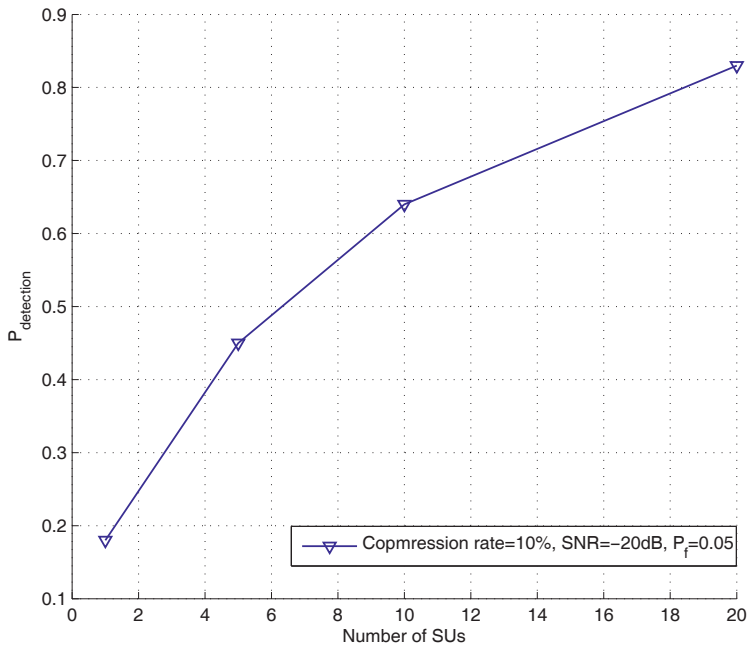

Figure 5.6: Probability of detection, P_D, vs. number of collaborative radios (SUs: secondary users) with compressed sensing of ratio $\frac{M}{N} = 10\%$ and Algebraic detection of order $P = 1$, at SNR$=-20dB$ and $P_F = 0.05$.

These results are obtained with Algebraic detection of order $P = 1$, where

increasing the order to $P = 2$ improves the performance dramatically, while complexity increases to $2M$ from M. But, still, for example for $\frac{M}{N} = 10\%$, complexity remains much less than complexity of ED, i.e., N.

As a final word, we can say that the collaborative compressed sensing decreases the complexity and energy consumption of cognitive radio networks remarkably due to the low sampling rate required for each radio while it makes the cognitive network robust against fading.

5.6 Conclusion

A new sensing technique which combines compressive sampling and an algebraic method for detecting spectrum holes in a UWB wireless sensor network scenario is presented. The designed measurement matrix and combination with algebraic detector satisfies the goal of reducing sampling complexity at sensor nodes and therefore enabling feedback in UWB wireless sensors network. The analysis of the complexity of the proposed technique shows that the complexity is dramatically reduced compared to the traditional algebraic detector, specially when the model order of the algebraic detector increases. In addition, the presented centralized collaborative sensing technique reduces complexity at each node even further and provides a better robustness to the system in fading conditions.

Chapter 6

Conclusion & Future Work

In this thesis several techniques for mitigating narrowband interference (NBI) in the context of ultra wideband (UWB) short range wireless sensor networks, specifically for biomedical application, are proposed.

In the context of *blind* UWB wireless sensor networks several proposals are provided to increase the system robustness against NBI. Where by *blind* we mean that the system has no information about NBI and its proximity for example by receiving feedback. The proposed multiband signaling scheme that is supported by frequency interleaving and error correcting coding suggests that the sensor network can tolerate existence of random NBI sources to some good extent. This method provides a great opportunity for multiuser scenarios, and thus we suggest a scheduling policy for multiuser scenario. The discovered scheduling policy, via Nash equilibrium, provides each user/sensor in the network with a fair access to the resources and keeps the system in a steady state, i.e., none of the users can gain more benefit for itself by deviating from the scheduling policy. In addition a new modulation, pulse position and frequency modulation (PPFM), is proposed that is able to inherently recover some errors that have occurred due to NBI. It is shown that PPFM with differential receiving algorithm mitigates strong NBI and performs better than a conventional system with pulse position modulation (PPM).

Providing UWB wireless sensor network with feedback is a great way to increase system robustness against NBI, although it introduces more complexity to the sensor nodes. Therefore, to keep complexity low at the sensor nodes, we proposed using compressed sensing (CS) with an algebraic detector which makes ultra wideband spectrum sensing possible. Combined detection is also suggested, and this improves robustness in fading conditions and it can also decrease complexity at each individual node more.

Overall, the thesis addresses the NBI problem in UWB wireless sensor networks by proposing different methods that are practical and have low complexity. Combination of the suggested methods are possible and this ability can provide practical solutions for increasing the system robustness in different conditions.

6.1 Future Work

An interesting direction to continue this work in the future is real implementation of the proposed methods in hardware. The hardware can be one of the existing platforms designed for testing different systems, for example universal software radio peripherals (USRP). Real implementation has its own challenges, good lessons, and it helps to further develop the methods. Furthermore, combination of the suggested techniques can be implemented and studied.

Bibliography

[1] Grzegorz Adamiuk, Jens Timmermann, Christophe Roblin, Wouter Dullaert, Philipp Gentner, Klaus Witrisal, Thomas FÃijgen, Ole Hirsch, Guowei Shen, Roberto Verdone, and Alberto Zanella. Pervasive mobile and ambient wireless communications. Signals and Communication Technology, pages 249–298. Springer London, 2012.

[2] G. R Aiello and G. D Rogerson. Ultra-wideband wireless systems. *Microwave Magazine, IEEE*, 4(2):36–47, June 2003.

[3] Arslan, Chen Zhi Ning, and Di Benedetto. *Ultra Wideband Wireless Communication*. Wiley, Newark, electronic version edition, 2006.

[4] H. Arslan. Cross-Modulation interference reduction for Pulse-Position modulated UWB signals. In *Vehicular Technology Conference, 2006. VTC-2006 Fall. 2006 IEEE 64th*, pages 1–5, 2006.

[5] Norman C. Beaulieu. Designing Ultra-Wide bandwidth (UWB) receivers for Multi-User interference environments, 2008.

[6] E. J. Candès. Compressive sampling. In *Proceedings of the International Congress of Mathematicians*, Madrid, Spain, 2006.

[7] E.J. Candes, J. Romberg, and T. Tao. Robust uncertainty principles: exact signal reconstruction from highly incomplete frequency information. *Information Theory, IEEE Transactions on*, 52(2):489–509, 2006.

[8] E.J. Candes and M.B. Wakin. An introduction to compressive sampling. *IEEE Signal Processing Magazine*, 25(2):21–30, March 2008.

[9] Emmanuel Candes, Justin Romberg, and Terence Tao. Stable signal recovery from incomplete and inaccurate measurements. *math/0503066*, March 2005.

[10] Emmanuel Candes and Terence Tao. Decoding by linear programming. *math/0502327*, February 2005.

[11] Emmanuel J. Candes and Terence Tao. Near-Optimal signal recovery from random projections: Universal encoding strategies? *IEEE Transactions on Information Theory*, 52(12):5406–5425, December 2006.

[12] C.F. Chiasserini and R.R. Rao. Coexistence mechanisms for interference mitigation in the 2.4-GHz ISM band. *Wireless Communications, IEEE Transactions on*, 2(5):964–975, 2003.

[13] Chia-Chin Chong, F. Watanabe, and H. Inamura. Potential of UWB technology for the next generation wireless communications. In *Spread Spectrum Techniques and Applications, 2006 IEEE Ninth International Symposium on*, pages 422 –429, August 2006.

[14] David Cypher. *Coexistence, Interoperability and Other Terms*. NIST, March 2000.

[15] B. Dang and T. Kaya. A low power wireless signal transmitter for biomedical Micro-Sensors. Ada, Ohio, 2012. American Society for Engineering Education.

[16] Q. H. Dang and A.-J. van der Veen. Narrowband interference mitigation for a transmitted reference ultra-wideband receiver. Florence, Italy, September 2006. Eusipco.

[17] N. Daniele, M. Pezzin, S. Derivaz, J. Keignart, and P. Rouzet. Principle and motivations of UWB technology for high data rate WPAN applications. Technical report, CiteSeerX, 2007.

[18] C. R.C.M daSilva and L. B Milstein. Spectral-Encoded UWB communication systems: Real-Time implementation and interference suppression. *Communications, IEEE Transactions on*, 53(8):1391–1401, August 2005.

[19] M A Davenport, M B Wakin, and R G Baraniuk. Detection and estimation with compressive measurements. Technical, Rice University, 2007.

[20] D.L. Donoho. Compressed sensing. *Information Theory, IEEE Transactions on*, 52(4):1289–1306, 2006.

[21] F. Dowla, F. Nekoogar, and A. Spiridon. Interference mitigation in transmitted-reference ultra-wideband (UWB) receivers. In *Antennas and Propagation Society International Symposium, 2004. IEEE*, volume 2, pages 1307–1310 Vol.2, 2004.

[22] M.F. Duarte, M.A. Davenport, M.B. Wakin, and R.G. Baraniuk. Sparse signal detection from incoherent projections. In *Acoustics, Speech and Signal Processing, 2006. ICASSP 2006 Proceedings. 2006 IEEE International Conference on*, volume 3, page III, 2006.

[23] FCC. Spectrum policy task force report. Technical report, November 2002.

[24] R.J. Fontana. A brief history of UWB communications. *Trans. Microwave Theory and Tech*, 14(11):528–547, 1966.

[25] R. Gagliardi. A geometrical study of transmitted reference communication systems. *Communication Technology, IEEE Transactions on*, 12(4):118 –123, December 1964.

[26] Matthew Gast. *802.11 Wireless Networks: The Definitive Guide*. O'Reilly Media, 2 edition, May 2005.

[27] O. V. Gonzalez and W. A. Moreno. Narrowband interference detection in multiband UWB systems. In *2005 IEEE/Sarnoff Symposium on Advances in Wired and Wireless Communication*, pages 160–163, 2005.

[28] W. Guibene, H. Moussavinik, and A. Hayar. Combined compressive sampling and distribution discontinuities detection approach to wideband spectrum sensing for cognitive radios. In *Ultra Modern Telecommunications and Control Systems and Workshops (ICUMT), 2011 3rd International Congress on*, pages 1 –7, October 2011.

[29] Wael GUIBENE, Monia TURKI, Aawatif HAYAR, and Bassem ZAYEN. Development and implementation of an algebraic detector for spectrum sensing. *submitted to IEEE Journal on Selected Areas in Communications: Special Issue on Advances in Cognitive Radio Networking and Communications*.

[30] Tiantian Guo, Luyong Zhang, Wei Liu, and Zheng Zhou. A novel solution to power problems in implanted biosensor networks. *Conference Proceedings: ... Annual International Conference of the IEEE Engineering in Medicine and Biology Society. IEEE Engineering in Medicine and Biology Society. Conference*, 1:5952–5955, 2006. PMID: 17945924.

[31] I. Guvenc and H. Arslan. On the modulation options for UWB systems. In *Military Communications Conference, 2003. MILCOM 2003. IEEE*, volume 2, pages 892–897 Vol.2, 2003.

[32] Ismail Güvenç, Sinan Gezici, and Zafer Sahinoglu. *Reliable Communications for Short-Range Wireless Systems*. Cambridge University Press, March 2011.

[33] M. Haddad, A. M Hayar, M. H Fetoui, and M. Debbah. Cognitive radio sensing information-theoretic criteria based. In *Cognitive Radio Oriented Wireless Networks and Communications, 2007. CrownCom 2007. 2nd International Conference on*, pages 241–244, 2007.

[34] S. Haykin. Cognitive radio: brain-empowered wireless communications. *Selected Areas in Communications, IEEE Journal on*, 23(2):201–220, 2005.

[35] Joseph Mitola Iii. *An Integrated Agent Architecture for Software Defined Radio*. Doctor of technology, Royal Inst. Technol. (KTH), Stockholm, Sweden, 2000.

[36] C. Kocks, A. Viessmann, M. Al-Olofi, Shangbo Wang, G. H Bruck, and P. Jung. Analysis of combined ultra-wideband systems. In *2011 International Conference on Communications, Computing and Control Applications (CCCA)*, pages 1–4. IEEE, March 2011.

[37] Lutz Lampe and Klaus Witrisal. Challenges and recent advances in IR-UWB system design. pages 3288–3291, June 2010.

[38] Lawrence Larson, David Laney, and Joe Jamp. An overview of hardware requirements for UWB systems: interference issues and transceiver design implications. 2:863– 867 Vol.2, October 2003.

[39] Chun Yi Lee and C. Toumazou. Ultra-low power UWB for real time biomedical wireless sensing. pages 57–60 Vol. 1, May 2005.

[40] Jin-Shyan Lee, Yu-Wei Su, and Chung-Chou Shen. A comparative study of wireless protocols: Bluetooth, UWB, ZigBee, and Wi-Fi. In *33rd Annual Conference of the IEEE Industrial Electronics Society, 2007. IECON 2007*, pages 46–51. IEEE, November 2007.

[41] Jiang Lei, Jianxin Guo, and Hou Jun. Study on coexisting interference detecting algorithm for Ultra-Wideband communications. pages 1–4. IEEE, September 2011.

[42] Huan-Bang Li. *Ultra-Wideband Technology and Its Standardization for Wireless Personal Area Networks*. National Institute of Information and Communications Technology (NICT), Japan, 2007.

[43] Zhendong Luo, Hong Gao, Yuanan Liu, and Jinchun Gao. A new UWB pulse design method for narrowband interference suppression. 6:3488–3492 Vol.6, December 2004.

[44] Xiaoli Lv and Fengming Bai. Review of Ultra-Wideband communication technology based on compressed sensing. *Procedia Engineering*, 29(0):3262–3266, 2012.

[45] R. K. Mallik, R. A. Scholtz, and G. Papavassilopoulos. A simple dynamic jamming game. In *IEEE International Symposium on Information Theory,. Proceedings.*, 1994.

[46] R. D McKelvey and T. R Palfrey. Quantal response equilibria for normal form games. *Games and Economic Behavior*, 10(1):6–38, 1995.

[47] Richard D. McKelvey, Andrew M. McLennan, and Theodore L. Turocy. Gambit: Software tools for game theory, version 0.2007.12.04., http://www.gambit-project.org, 2007.

[48] V.P. Mhatre, K. Papagiannaki, and F. Baccelli. Interference mitigation through power control in high density 802.11 WLANs. In *INFOCOM 2007. 26th IEEE International Conference on Computer Communications. IEEE*, pages 535–543, 2007.

[49] H. Moussavinik and I. Balasingham. Interference mitigation using pulse position and frequency modulation for multiband systems. In *Industrial Electronics Applications (ISIEA), 2010 IEEE Symposium on*, pages 176 –180, October 2010.

[50] H. Moussavinik, I. Balasingham, and T. Ramstad. Handling unknown NBI in IR-UWB system used in biomedical wireless sensor networks. 1:177–180, September 2008.

[51] H. Moussavinik, S. Byun, and I. Balasingham. On the steady state in multiuser multiband IR-UWB without NBI detection. In *Wireless Communication Systems, ISWCS. IEEE International Symposium on*, September 2009.

[52] H. Moussavinik, W. Guibene, and A. Hayar. Centralized collaborative compressed sensing of wideband spectrum for cognitive radios. In *Ultra Modern Telecommunications and Control Systems and Workshops (ICUMT), 2010 International Congress on*, pages 246 –252, October 2010.

[53] Hessam Moussavinik. *TPC Iterative Decoding with Flooding and Row-Column Updating Schedule*. Number 2006:48 in Ex / Institutionen för signaler och system, Chalmers tekniska högskola. Chalmers tekniska högskola, Göteborg, 2006.

[54] Hessam Moussavinik, Sang-Seon Byun, and Ilangko Balasingham. Towards robustness in multiband/multiuser IR-UWB: overcoming unknown NBI via FEC and subband scheduling. In *Proceedings of the 11th international conference on Advanced Communication Technology - Volume 3*, ICACT'09, pages 1947–1949, Piscataway, NJ, USA, 2009. IEEE Press. ACM ID: 1701745.

[55] Ian Oppermann, Matti Hämäläinen, and Jari Iinatti. *UWB: Theory and Applications*. Wiley, November 2004.

[56] M. J Osborne and A. Rubinstein. *A course in game theory*. MIT press, 1999.

[57] Mitsugu Otsu, Ryohei Nakamura, and Akihiro Kajiwara. Elderly-care monitoring sensor using stepped-FM UWB scheme. In *2012 IEEE Sensors Applications Symposium (SAS)*, pages 1–4. IEEE, February 2012.

[58] B. Parr, ByungLok Cho, K. Wallace, and Zhi Ding. A novel ultra-wideband pulse design algorithm. *Communications Letters, IEEE*, 7(5):219–221, May 2003.

[59] D. Porcino and W. Hirt. Ultra-wideband radio technology: potential and challenges ahead. *IEEE Communications Magazine*, 41(7):66–74, July 2003.

[60] Z. Quan, S. Cui, H. V. Poor, and A. H. Sayed. Collaborative wideband sensing for cognitive radios. *IEEE Signal Processing Magazine*, 25(6):60–73, 2008.

[61] First Report and Order. Revision of part 15 of the commission's rule regarding ultra-wideband transmission system FCC 02-48. 2002.

[62] Montserrat Ros, Joshua Boom, Gavin de Hosson, and Matthew D'Souza. Indoor localisation using a Context-Aware dynamic position tracking model. *International Journal of Navigation and Observation*, 2012:1–12, 2012.

[63] A. Sahai and D. Cabric. A tutorial on spectrum sensing: fundamental limits and practical challenges. In *Proc. IEEE Symposium on New Frontiers in Dynamic Spectrum Access Networks (DySPAN)*, November 2005.

[64] Henrik Schulze and Christian Lueders. *Theory and Applications of OFDM and CDMA: Wideband Wireless Communications*. John Wiley & Sons, December 2005.

[65] Loren Schwiebert, Sandeep K. S Gupta, and Jennifer Weinmann. Research challenges in wireless networks of biomedical sensors. In *Proceedings of the 7th annual international conference on Mobile com-*

puting and networking, MobiCom '01, pages 151–165, New York, NY, USA, 2001. ACM. ACM ID: 381692.

[66] Ehab M. Shaheen and Mohamed El-Tanany. Analysis and mitigation of the narrowband interference impact on IR-UWB communication systems. *Journal of Electrical and Computer Engineering*, 2012:1–8, 2012.

[67] Hua Shao and Norman C. Beaulieu. Direct sequence and Time-Hopping sequence designs for narrowband interference mitigation in impulse radio UWB systems. *IEEE Transactions on Communications*, 59(7):1957–1965, July 2011.

[68] Xuemin Shen, Mohsen Guizani, Robert Caiming Qiu, and Tho Le-Ngoc. *Ultra-Wideband Wireless Communications and Networks*. Wiley-Blackwell, February 2006.

[69] Xiaolin Shi. UWB waveform design method for narrowband interference suppression based on raised cosine pulse. pages 646–649. IEEE, June 2011.

[70] Keisuke Sodeyama and Ryuji Kohno. Low duty-cycle UWB communications design for body area network. In *Proceedings of the First ACM MobiHoc Workshop on Pervasive Wireless Healthcare*, MobileHealth '11, pages 2:1–2:5, New York, NY, USA, 2011. ACM.

[71] Hamza Soganci, Sinan Gezici, and H. Poor. Accurate positioning in ultra-wideband systems. *IEEE Wireless Communications*, 18(2):19–27, April 2011.

[72] Z. Tian and G. B Giannakis. A wavelet approach to wideband spectrum sensing for cognitive radios. In *Cognitive Radio Oriented Wireless Networks and Communications, 2006. 1st International Conference on*, pages 1–5, 2006.

[73] Zhi Tian and G.B. Giannakis. Compressed sensing for wideband cognitive radios. In *Acoustics, Speech and Signal Processing, 2007. ICASSP 2007. IEEE International Conference on*, volume 4, pages IV–1357–IV–1360, 2007.

[74] Joel A. Tropp and Anna C. Gilbert. Signal recovery from random measurements via orthogonal matching pursuit. *IEEE Transactions on Information Theory*, 53(12):4655–4666, December 2007.

[75] T. L Turocy. A dynamic homotopy interpretation of the logistic quantal response equilibrium correspondence. *Games and Economic Behavior*, 51(2):243–263, 2005.

[76] H. Urkowitz. Energy detection of unknown deterministic signals. *Proceedings of the IEEE*, 55(4):523–531, 1967.

[77] Hirt W. Ultra-wideband radio technology: overview and future research. *Computer Communications*, 26(1):46–52, 2003.

[78] Y. Wang, X. Dong, and I. J. Fair. Spectrum shaping and NBI suppression in UWB communications. *IEEE Transactions on Wireless Communications*, 6(5):1944–1952, 2007.

[79] M.Z. Win and R.A. Scholtz. Impulse radio: how it works. *Communications Letters, IEEE*, 2(2):36 –38, February 1998.

[80] Wen-Bin Yang and Kamran Sayrafian-Pour. Interference mitigation for body area networks. pages 2193–2197. IEEE, September 2011.

[81] B. Zayen, A. Hayar, and K. Kansanen. Blind spectrum sensing for cognitive radio based on signal space dimension estimation. In *IEEE International Conference on Communications*, pages 14–18, June 2009.

[82] B. Zayen, A.M. Hayar, and D. Nussbaum. Blind spectrum sensing for cognitive radio based on model selection. In *Cognitive Radio Oriented Wireless Networks and Communications, 2008. CrownCom 2008. 3rd International Conference on*, pages 1–4, May 2008.

[83] Guiying Zhang, Yujie Dai, Xiaoxing Zhang, Yingjie Lv, and Liying Chen. Design and implementation of UWB pulse with multiple narrow-band interferences mitigation. pages 1154–1157. IEEE, April 2011.

[84] Li Zhang, Hao Zhang, Xue Rong Cui, and T Aaron Gulliver. Ultra wideband indoor positioning using kalman filters. *Advanced Materials Research*, 433-440:4207–4213, January 2012.

[85] Zhi Zhang, Zhonghai Lu, Qiang Chen, Xiaolang Yan, and LiRong Zheng. Code division multiple access/pulse position modulation ultra-wideband radio frequency identification for internet of things: concept and analysis. *International Journal of Communication Systems*, 25(9):1103–1121, September 2012.

[86] Li Zhao and A.M. Haimovich. Capacity of m-ary PPM ultra-wideband communications over AWGN channels. In *Vehicular Technology Conference, 2001. VTC 2001 Fall. IEEE VTS 54th*, volume 2, pages 1191–1195, 2001.

Appendix A

UWB Pulse Design Algorithm

This appendix presents the used UWB pulse design algorithm as proposed in [58].

Given a desired frequency mask $H(f)$, the pulse design algorithm utilizes its corresponding impulse response $h(t)$. The aim is to design a pulse signal $\psi(t)$ that is time-limited to T_m seconds (impulse pulse period) while exhibiting minimal distortion as it passes through the filter with impulse response $h(t)$, as shown in Figure A.1. In other words, when the pulse $\psi(t)$ is sent through the filter $h(t)$, the filter output should be $\lambda\psi(t)$, where λ is an attenuation factor.

If $p(t)$ is the pulse shape, $\psi(t)$ has the following form:

$$\psi(t) = \begin{cases} p(t) & |t| < \frac{T_m}{2} \\ 0 & \text{elsewhere} \end{cases} . \tag{A.1}$$

Then,

$$\lambda\psi(t) = \int_{-\infty}^{\infty} \psi(\tau)h(t-\tau)\,\mathrm{d}\tau = \int_{\frac{-T_m}{2}}^{\frac{T_m}{2}} \psi(\tau)h(t-\tau)\,\mathrm{d}\tau. \tag{A.2}$$

By sampling at a rate of N samples per pulse period T_m, (A.2) can be expressed as following:

$$\lambda\psi[n] = \sum_{m=-\frac{N}{2}}^{\frac{N}{2}} \psi[m]h[n-m],\ n = -\frac{N}{2} \cdots \frac{N}{2} \tag{A.3}$$

where n and m take on integer values only.
Upon expressing (A.3) in vector form, the convolution in (A.2) becomes a matrix multiplication of a $(N+1) \times (N-1)$ Toeplitz matrix H with the sample vector ψ such as

$$\lambda \underbrace{\begin{pmatrix} \frac{\psi[-N}{2]} \\ \frac{\psi[-N}{2+1]} \\ \vdots \\ \psi[0] \\ \vdots \\ \frac{\psi[N}{2]} \end{pmatrix}}_{\psi} = \underbrace{\begin{pmatrix} h[0] & h[-1] & \cdots & h[-N] \\ h[1] & h[0] & \cdots & h[-N+1] \\ \vdots & \vdots & \cdots & \vdots \\ \frac{h[N}{2]} & \frac{h[N}{2-1]} & \cdots & \frac{h[-N}{2]} \\ \vdots & \vdots & \cdots & \vdots \\ h[N] & h[N-1] & \cdots & h[0] \end{pmatrix}}_{\mathbf{H}} \times \underbrace{\begin{pmatrix} \frac{\psi[-N}{2]} \\ \frac{\psi[-N}{2+1]} \\ \vdots \\ \psi[0] \\ \vdots \\ \frac{\psi[N}{2]} \end{pmatrix}}_{\psi} \tag{A.4}$$

Clearly ψ is an eigenvector of $\mathbf{H}$. Thus, we define ψ as $|\psi_1, \psi_2, \cdots, \psi_m|$ and Λ as the $(\lambda_1, \lambda_2, \cdots, \lambda_m)$, where the eigenvalues are arranged in descending order, i.e., $\lambda_1 > \lambda_2 > \cdots > \lambda_m$. Every numerical solution of (A.2) can be found by means of eigenvalues decomposition.
Each eigenvalue is related to the percentage of its corresponding eigenvector's power concentrated inside the desired frequency mask $H(f)$. The

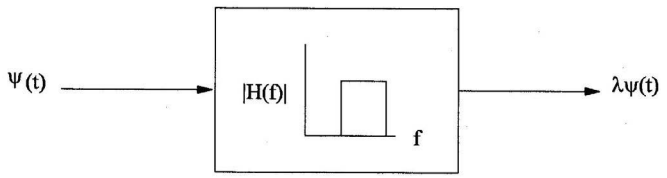

Figure A.1: Block diagram of pulse design algorithm [58].

greater the eigenvalue, the better the power spectrum fits. Therefore, only the eigenvectors corresponding to large eigenvalues should be taken as pulse designs and selected for implementation.
Example pulses are given for a bandpass frequency mask between 3.1 GHz and 10.6 GHz represented in the frequency domain by (A.5) and in the time domain by (A.6), where $f_L = 3.1$ GHz and $f_U = 10.6$ GHz.

$$H(f) = \begin{cases} 1, & 3.1\text{GHz} < f < 10.6\text{GHz} \\ 0, & \text{elsewhere} \end{cases} . \tag{A.5}$$

$$h(t) = 2f_U \text{sinc}(2f_U t) - 2f_L \text{sinc}(2f_L t). \tag{A.6}$$

Having $N = 64$ and $T_m = 1$ ns, corresponding eigenvectors to two relatively large eigenvalues are suggested for UWB pulse designs as plotted in Figure A.2. The power spectra of these pulses, Figure A.3, show that the majority of their power is concentrated in the desired frequency band, and they comply with the FCC regulations.

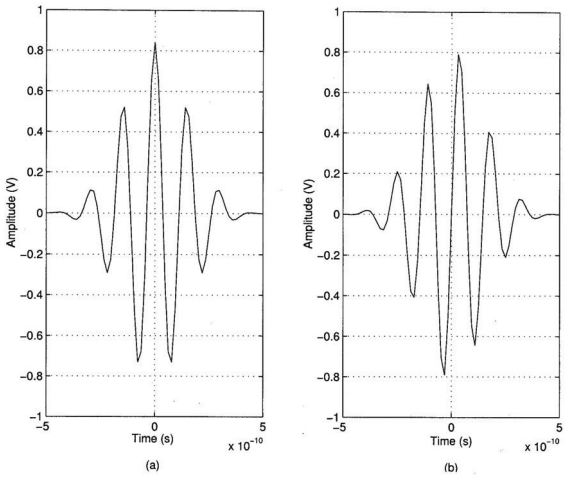

Figure A.2: Pulse shapes obtained from the pulse design algorithm using a single bandpass frequency mask (a) $\psi_1(t)$, (b) $\psi_2(t)$ [58].

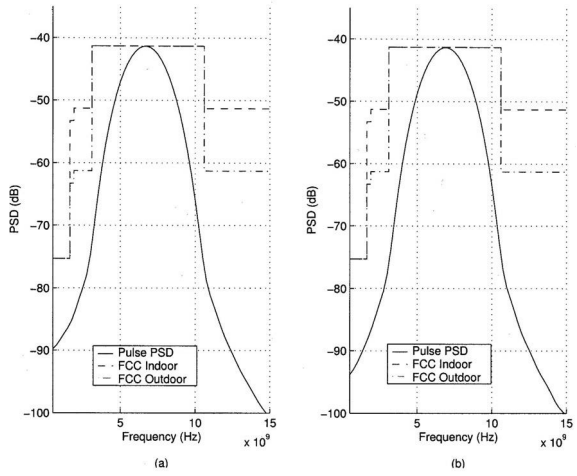

Figure A.3: Power spectra of pulse shapes obtained from the pulse design algorithm using a single bandpass frequency mask (a) $\psi_1(f)$, (b) $\psi_2(f)$ [58].